

# DESIGN OF DAMPING CONTROLLER FOR CSI STATCOM

## A DISSERTATION

*Submitted in partial fulfillment of the  
requirements for the award of the degree*

*of*

**MASTER OF TECHNOLOGY**

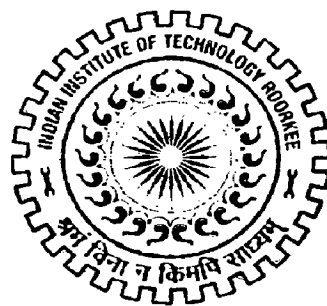
*in*

**ELECTRICAL ENGINEERING**

**(with Specialization in Power Systems Engineering)**

By

**NILESH**



**DEPARTMENT OF ELECTRICAL ENGINEERING  
INDIAN INSTITUTE OF TECHNOLOGY ROORKEE  
ROORKEE -247 667 (INDIA)  
JUNE, 2007**

## **CANDIDATE'S DECLARATION**

---

I hereby declare that the work presented in this dissertation entitled "**Design of Damping Controller for CSI STATCOM**" submitted in partial fulfillment of the requirements for the award of the Master of Technology with specialization in the Power System Engineering in the Department of Electrical Engineering, Indian Institute of Technology, Roorkee, Roorkee. The work is carried out during the period from August 06 to June 07 under the guidance of Dr. B. Das, Associate Professor and Dr. V. Pant, Asst. Professor, Department of Electrical Engineering, Indian Institute of Technology, Roorkee, Roorkee.

I have not submitted the matter embodied in this dissertation for the award of any degree or diploma.

Date: 29/06/07

Nilesh

Place: Roorkee

NILESH

---

## **CERTIFICATE**

This is to certify that the above statement made by the candidate is true to the best of my knowledge and belief.



**(Dr. VINAY PANT)**

Asst. Professor,  
Department of Electrical Engineering,  
Indian Institute of Technology,  
Roorkee-247667,  
India.



**(Dr. B. DAS)**

Associate Professor  
Department of Electrical Engineering,  
Indian Institute of Technology,  
Roorkee-247667,  
India.

## ACKNOWLEDGEMENT

I have great pleasure in expressing my deep sense of gratitude to Dr. Biswaroop Das and Dr. Vinay Pant, Electrical Engineering Department, IIT Roorkee, for their keen interest, invaluable guidance and generous help throughout the preparation of this dissertation. It was very pleasant and inspiring experience for me to work under their able guidance.

I also acknowledge the blessings of my parents and cooperation of my friends which is very invaluable to me.

## ABSTRACT

---

For reliable service, a power system must remain intact and be capable of withstanding a wide variety of disturbances. Therefore, it is essential that the system should be designed with proper precautions so that it can tolerate the more probable as well as most adverse contingencies. As, we know the stability problem involves the rotor angle oscillations which is natural in power systems. If the oscillations are severe one, the synchronous machine may out of step from the rest of the system.

This thesis work deals with a power system installed with a current source inverter based static synchronous compensator and demonstrates its effectiveness in damping out the rotor oscillations. A Phillip-Heffron model of single machine infinite bus power system installed with a CSI STATCOM was developed which is actually a linearization around the operating point. This model acts as the basis for a state feedback controller which actually gives us a way to place the closed system poles at the most suitable place. The whole work was done in MATLAB package and the results show a very nice damped system.

Finally a practical CSI STATCOM was simulated in PSCAD/EMTDC package to find out its capabilities with active as well as passive filters both. Switching scheme adopted was tri logic pulse width modulation scheme. It was found that CSI STATCOM installed with the passive filter in a small size power system gives the required results but an active filter in a large size power system need some further modifications.

## CONTENTS

		Pages
<b>CANDIDATE'S DECLARATION</b>		i
<b>CERTIFICATE</b>		i
<b>ACKNOWLEDGEMENT</b>		ii
<b>ABSTRACT</b>		iii
<b>LIST OF FIGURES</b>		vi
<b>LIST OF TABLES</b>		viii
<b>CHAPTER 1</b>	<b>CURRENT SOURCE INVERTER BASED STATCOM: A BIRD'S EYE VIEW</b>	
	1.1 CSI VERSUS VSI	1
	1.2 WORKING PRINCIPLE OF A CURRENT SOURCE INVERTER BASED STATCOM	3
	1.3 LITERATURE REVIEW	5
<b>CHAPTER 2</b>	<b>PHILLIPS-HEFFRON MODEL OF POWER SYSTEM INSTALLED WITH CSI STATCOM</b>	
	2.1 DERIVATION AND LINEARIZATION OF STATE EQUATIONS	7
	2.2 DERIVATION AND LINEARIZATION OF OUTPUT EQUATIONS	13
<b>CHAPTER 3</b>	<b>CONTROLLER DESIGN</b>	
	3.1 CONCEPT OF STATE-FEEDBACK CONTROLLER	17
	3.2 POLE PLACEMENT BY STATE FEEDBACK	17
	3.3 CONTROL STRATEGY FOR THE CSI STATCOM DAMPING CONTROLLER	19
	3.4 MATLAB COMMAND FOR POLE PLACEMENT	19
	3.5 CALCULATION OF CONTROLLER GAIN MATRIX	19
	3.6 OBSERVER DESIGN	20
	3.6.1 PROCEDURE OF SELECTION OF STABILIZING OUTPUT SIGNAL FOR STATCOM	20
	3.6.2 CHOICE OF OUTPUT SIGNAL	22
	3.7 NON LINEAR SIMULATIONS	24

3.7.1	INITIAL VALUE CALCULATION	24
3.7.2	DIFFERENTIAL AND ALGEBRAIC EQUATIONS	25
3.7.3	PLOTS	26
3.8	DISCUSSION ON RESULTS:	27
<b>CHAPTER 4</b>	<b>CSI STATCOM IMPLEMENTATION IN PSCAD</b>	
4.1	BASIC CONFIGURATION OF A CURRENT SOURCE INVERTER	28
4.2	SWITCHING SCHEME FOR THE INVERTER	28
4.2.1	PRACTICAL IMPLEMENTATION & THE TRAJECTORY TAKEN BY THE TRI-LOGIC PWM	29
4.2.2	TRANSLATION OF $X_j$ TO $Y_j$	29
4.2.3	INTERPRETATION OF VALUE OF $Y_j(t)$	30
4.2.4	CONTIGUOUS STATE NETWORK	32
4.2.5	SIMULATION STUDY	32
4.2.6	TRANSITION BETWEEN SUB PERIODS	34
4.2.7	DESIGNING THE GATING SEQUENCE OF VALVES	34
4.3	SIMULATION OF CURRENT SOURCE INVERTER	35
4.3.1	PROGRAMMING LOGIC	35
4.3.2	CIRCUIT PARAMETERS	37
4.3.3	OUTPUT WAVEFORMS	37
4.4	CASE STUDY	38
4.5	ACTIVE FILTER	39
4.5.1	d-q-o TRANSFORMATION	40
4.5.2	HIGH PASS FILTER	42
4.5.3	HYSTERESIS CURRENT CONTROL	42
4.5.4	STRATEGY OF THE ACTIVE FILTER	43
4.5.5	RESULTS: EFFECTIVENESS OF ACTIVE FILTER	44
4.6	DISCUSSION ON RESULTS	44
	<b>CONCLUSION AND SCOPE FOR FURTHER WORK</b>	<b>46</b>
	<b>REFERENCES</b>	<b>47</b>
	<b>APPENDIX-A</b>	<b>49</b>
	<b>APPENDIX-B</b>	<b>50</b>

## LIST OF FIGURES

		page
Figure 1.1	Vector diagram of CSI based STATCOM	5
Figure 1.2	Schematic diagram of CSI based STATCOM	5
Figure 2.1	A CSI STATCOM installed in a single machine infinite-bus power system	7
Figure 2.2	Exciter block diagram	9
Figure 3.1	Phasor dia. of system	24
Figure 3.2	Rotor angle oscillations	26
Figure 3.3	Rotor speed oscillation	26
Figure 3.4	Variation of $E_q'$	26
Figure 3.5	Variation of $E_{fd}$	26
Figure 3.6	Variation of $I_{dc}$	26
Figure 3.7	Comparision of system stability for $P_e = 1.1$ pu	27
Figure 4.1	Circuit diagram of current source inverter	28
Figure 4.2	Single switching actions & contiguous states of state #2	32
Figure 4.3	Contiguous states of 6-valve current source converter	32
Figure 4.4	$Y_j$ waveforms	33
Figure 4.5	Flow chart for programming logic of component ' <i>TLG_SWITCHING</i> '	36
Figure 4.6	Current waveform before the filter in phase A	37
Figure 4.7	Current waveform after the filter in phase A	37
Figure 4.8	Compensated power system	38
Figure 4.9	Phase angle control strategy	38
Figure 4.10	Variation of bus voltage	38
Figure 4.11	Variation of bus reactive power	38
Figure 4.12	Voltage profile for A-B-C-G fault	39
Figure 4.13	Circuit diagram of active filter	40
Figure 4.14	Functional block diagram of active filter	40

Figure 4.15	Principle of hysteresis band current control	43
Figure 4.16	Voltage rise and current waveform	44



## LIST OF TABLES

---

		pages
Table 4.1	Truth table of translations	30
Table 4.2	Current source converter states	31
Table 4.3	Sequence of tri logic states	33
Table 4.4	Voltages during the faults	45

# CHAPTER 1

---

## CURRENT SOURCE INVERTER BASED STATCOM: A BIRD'S EYE VIEW

### INTRODUCTION:

Static synchronous compensator or STATCOM is an analogous of synchronous condenser. It is realized by an energy storing source connected to an inverter which is finally connected to grid. The energy storing source may be a battery or a capacitor or an inductor. In case of inductor, it is called current source inverter based STATCOM. Since it has no rotating parts, its response is much faster than synchronous condenser. There are some other superior qualities of a STATCOM which are listed below [1], [2]:

- (a) Power transfer limit is doubled.
- (b) Voltage support to prevent voltage instability
- (c) Improvement of transient stability margin
- (d) Enhancement of power oscillation damping

### 1.1 CSI VERSUS VSI:

STATCOM has been at the center of attention and the subject of active research for many years but the focus of all the published work on STATCOM has been on using Voltage Source Inverter topology. The reasons behind the choice of VSI over CSI are as follows [3].

1. More costly: To get sinusoidal output current filter capacitors are used at the ac terminals of a CSI. Hence power and control circuits of a CSI are more complex than a VSI. This makes CSI more costly.
2. Harmonic distortion: Some harmonic components of output current may be amplified due to the resonance caused by ac side inductor & filter capacitors, causing high harmonic distortion in the ac-side current.
3. Requirement of additional diode: Unless, A diode has to be placed in series with each of the switches in CSI so as to our switches may have sufficient

reverse voltage withstanding capability or a switch of such as Gate-Turn-Off Thyristor (GTO) is used. This almost doubles the conduction losses compared with the case of VSI.

4. Higher Losses: The dc-side energy-storage element in VSI topology is a capacitor, whereas that in CSI topology is an inductor. The power loss of an inductor is larger than that of a capacitor. Thus, the efficiency of a CSI is lower than that of a VSI.

As a result of the recent developments in the control of CSI and the technology of semiconductor switches, the above situation is likely to change for the following reasons [3]:

1. The presence of the ac-side capacitors makes both voltage and current waveforms at the output terminals of CSI good sinusoids. The capacitors are the inherent filter for the CSI. Although a 48-pulse VSI STATCOM does not require a filter, the cost of the filter is transferred to the cost of multi-converters and multi-winding transformer.
2. A CSI STATCOM can be operated less than 900 Hz of switching frequency with a single converter. This reduces the filtering requirements compared with the case of a VSI as additional filter has to be used in a VSI STATCOM if operating at a lower frequency.
3. Careful design of the filter capacitors and introduction of sufficient damping using proper control methods can overcome the problem of the resonance between the capacitances and inductances on the ac-side.
4. Integrated Gate Commutated Thyristor (IGCT) is the optimum combination of the characteristics demanded in high-power applications. High ratings, high reverse voltage blocking capability, low snubber requirements, lower gate-drive power requirements than GTO and higher switching speed than GTO.
5. The dc-side losses are can to be minimized if superconductive materials are used in the construction of the dc-side reactor.

There are some features that make CSI STATCOM more beneficial than VSI STATCOM [3], [4]:

1. The magnitudes of the harmonic components in both converters are directly proportional to the magnitudes of the fundamental components of their direct output quantities. Under normal operating conditions, the current injected by STATCOM is a small percentage of the line current. Thus, when CSI is used, the current harmonics are also small. But, when VSI is used, for a small injected current, the output voltage of VSI is large and very close to the system voltage. This results in large voltage harmonics, leading to current harmonics that are larger than those generated by CSI, and thus more costly to filter.
2. When a VSI is used to inject reactive power to the system, the dc-side voltage must be larger than the peak value of the system line-to-line voltage so that the reactive power can be transferred between the STATCOM and the transmission line. While in case of the CSI based STATCOM, the dc-side current is just larger than the peak value of the required injected current which is a small percentage of the line current. This means that the dc energy storage requirement of CSI is lower than that of VSI when used to realize a STATCOM.
3. The CSI has an implicit short circuit protection. The rate of rise of fault current during external or internal faults is limited by the dc reactor in CSI. For VSI, the capacitor discharge current would rise very rapidly & can damage the valves.

## **1.2 WORKING PRINCIPLE OF A CURRENT SOURCE INVERTER BASED STATCOM [5]:**

The regulated reactive power at the connection point can be inductive or capacitive depending on the phase relationship of injected current with respect to the voltage at the connection point and the magnitude of reactive current can be regulated by a slight increase or decrease of the firing angle from the  $-90^\circ$  or  $+90^\circ$  position.

The relationship of injected current to active and reactive power can be explained by Fig. 1.1 and the schematic diagram of a CSI based STATCOM is shown in Fig. 1.2. If the compensator current  $I_{ac}$  has a  $90^\circ$  phase lag with respect to the terminal voltage  $V_T$ , the power system supplies reactive power to the compensator. On the other hand, if the

compensator current  $I_{ac}$  has a  $90^\circ$  phase lead with respect to the terminal voltage  $V_T$ , the compensator supplies reactive power to the power system. If the firing angle is larger than  $90^\circ$ , the compensator absorbs the active power from the power system and increases the dc reactor current. On the other hand, if the firing angle is smaller than  $90^\circ$ , the compensator supplies the active power to the power system and decreases the dc reactor current.

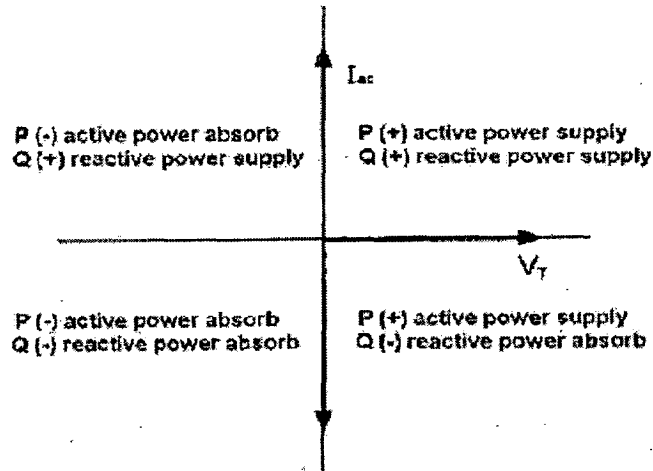


Figure 1.1: Vector diagram of CSI based STATCOM

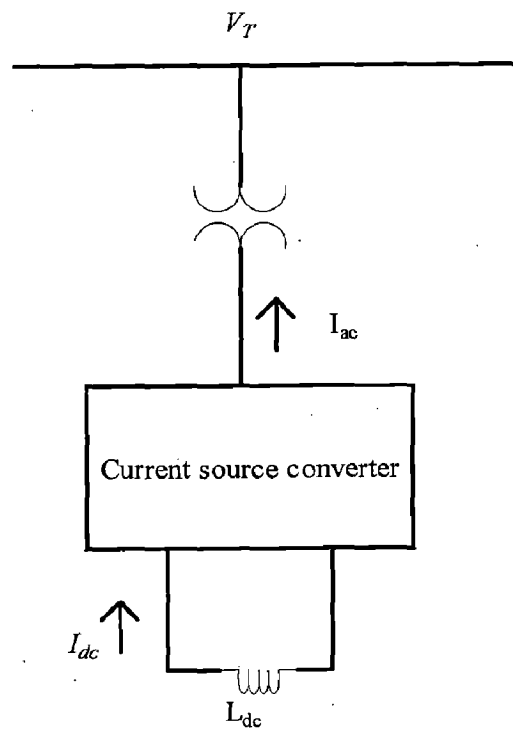


Figure 1.2: Schematic diagram of CSI based STATCOM

### 1.3 LITERATURE REVIEW

This paper [1] by Laszlo Gyugyi gives not only the basics of a STATCOM but also describes the dynamic compensation and real time control of power flow in transmission systems. It develops a comprehensive treatment of power flow control using solid-state synchronous voltage sources for shunt compensation, series compensation, and phase angle control.

This book [2] was written by the father of FACTS devices Narain Hingorani and Laszlo Gyugi. In fact this book is a 'Gold mine' where construction and operation of almost each and every FACTS device is described in full length. The complete theoretical aspect of STATCOM is discussed in magnificent way.

Yang Ye, Mehrdad Kazerani and Victor H. Quintana propose [3] a CSI STATCOM which generates a controllable current directly at its output terminals. It gives not only the reasons behind previously preferred VSI over CSI but also says why the recent developments in the control of CSI and the technology of semiconductor switches made CSI more effective than VSI. It gives a nice way to understand the d-q modeling of CSI STATCOM.

In this paper [4], Mehrdad Kazerani and Yang Ye compared the voltage and current-source inverter topologies from different viewpoints as: device rating, dc-side energy storage requirement, ac-side waveform quality, start-up, and cost. It finally deduced that current-source converter topology is gaining ground in competition with the voltage-source converter topology in high-power applications, including FACTS controllers.

B. M. Han & S. I. Moon, in his work [5], have given a very easy explanation of working of a CSI STATCOM.

In this work [6] H. F. Wang has established a linearized Phillips-Heffron model of a power system installed with a VSI STATCOM and demonstrates the application of the model in analyzing the damping effect of the STATCOM and designing a STATCOM stabilizer to improve power system oscillation stability.

This book [7] is of another giant of electrical engineering P. Kundur. He has elaborated each aspect of power system i.e. modeling of synchronous machines, exciters, turbines etc and finally found how they contribute in system stability.

This book [8] by M. Gopal presents the complete, modeling analysis and design of a control system; especially it puts light design on state feedback control system by proper pole placement.

This paper [9] by Dong Shen and P. W. Lehn throws light on traditional PI controllers as well as a fast ac current control inner loop and a slower dc current control outer loop. The inner loop, which is a combination of multivariable full state feedback and integral control, allows for rapid non-oscillatory dynamics of the ac current without overshoot or steady-state error.

M. M. Farsangi, in this paper [10], highlighted the importance of identifying the most effective input signals for damping the oscillations for the FACTS devices in a power system. Hankel singular values as well as right half plane zeros are used as indicator in SISO systems.

The paper [11] by Xiao Wang and Boon-Teck Ooi, describes a general method of translating three-phase bilogic PWM signals to three-phase trilogic PWM signals. It gives a complete understanding about the implementation of the Gating logic.

A 27-bus power system has been taken from this paper [12] by Biswarup Das and Bikash C. Pal.

Bimal K. Bose basically devoted his book [13] to AC drives, but the different PWM techniques for inverters were discussed in a very detailed manner.

This paper [14] gives a good understanding of a practical CSI var compensator. It describes the working and design of power as well as control circuits.

The first industry application of a CSC STATCOM with selective harmonic elimination, designed for group compensation of electric excavators is presented in the paper [15]. H.F. Bilgin, M. Ermis, K.N. Kose, A. Cetin, I. Cadirci, A. Acik, A. Terciyanli, C. Kocak, and M. Yorukoglu fairly described the operating principles, power stage, and design of dc link and the input filter.

This project work [16] by Bingsen Wang is completely devoted to the design of each and every component of a practical CSI STATCOM as well as the power system.

## CHAPTER 2

### PHILLIPS-HEFFRON MODEL OF POWER SYSTEM INSTALLED WITH CSI STATCOM

In this chapter the Phillips-Heffron model of power system installed with a CSI STATCOM has been developed. This model is a state space model which has been derived by the linearization of differential equations. For this purpose, in this work the assumptions taken have been taken as [6]:

- The whole system i.e. generator, transmission lines and the STATCOM are lossless.
- Current injected by the STATCOM is purely sinusoidal i.e. harmonic generation is nil.

#### 2.1 DERIVATION AND LINEARIZATION OF STATE EQUATIONS

In Fig 2.1 a single machine infinite-bus power system installed with a CSI STATCOM is shown. The STATCOM consists of a step down transformer (SDT), a three phase GTO based current source inverter and a DC inductor.

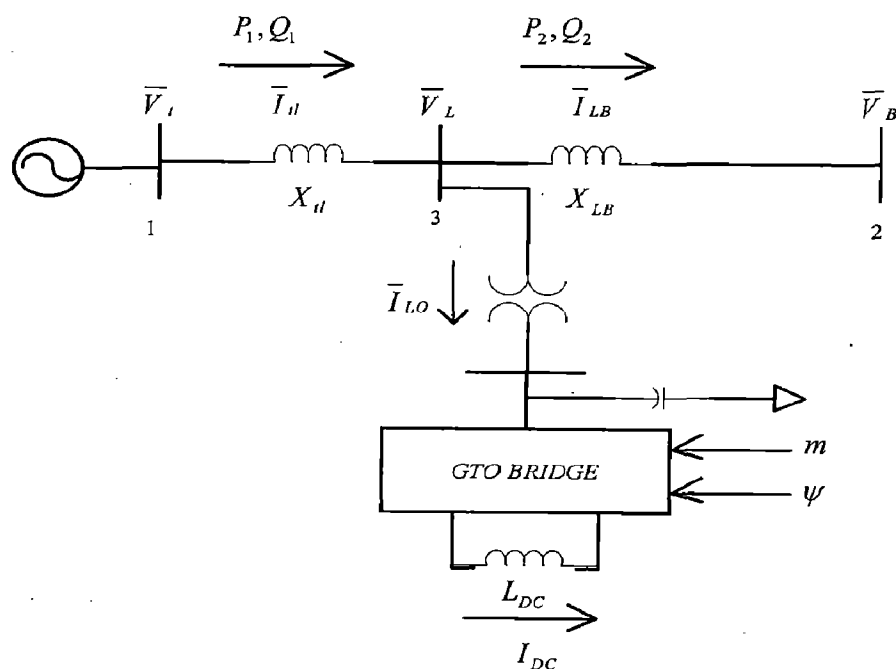


Figure 2.1: A CSI STATCOM installed in a single machine infinite-bus power system



The CSI generates a controllable AC current source

$$i_o(t) = I_o \sin(\omega t + \psi) = cI_{dc} \sin(\omega t + \psi) \quad (2.1)$$

Where, for the PWM inverter,  $c = mk$  and  $k$  is the ratio between AC and DC voltages, depending on the structure of the inverter;  $m$  is the modulation index defined by the PWM and phase  $\psi$  is defined by PWM.

We have, in phasor notation,

$$I_{LO} = cI_{dc}(\cos \psi + j \sin \psi) = cI_{dc} \angle \psi \quad (2.2)$$

Taking d and q components we have

$$I_{LOd} = cI_{dc} \cos \psi \quad (2.3)$$

$$I_{LOq} = cI_{dc} \sin \psi \quad (2.4)$$

We know

$$\bar{E}_I = \bar{E}_q' + j(X_d - X_d')I_{ld} \quad \text{And}$$

$$\bar{E}_q = \bar{E}_I - j(X_d - X_q)I_{ld} = \bar{E}_q' - jX_d'I_{ld} + jX_qI_{ld}$$

So, the terminal voltage

$$\begin{aligned} \bar{V}_t &= \bar{E}_q - jX_q\bar{I}_{ll} = \bar{E}_q - jX_qI_{ld} + X_qI_{lq} \\ &= \bar{E}_q' - jX_d'I_{ld} + jX_qI_{ld} - jX_qI_{ld} + X_qI_{lq} \\ &= X_qI_{lq} + j(E_q' - X_d'I_{ld}) \end{aligned} \quad (2.5)$$

Now from Fig 2.1,

$$\begin{aligned} \bar{I}_{ll} &= \frac{\bar{v}_L - \bar{v}_b}{jX_{LB}} + \bar{I}_{Lo} = \frac{\bar{v}_t - jX_{ll}\bar{I}_{ll} - \bar{v}_b}{jX_{LB}} + \bar{I}_{Lo} \\ \Rightarrow \bar{I}_{ll} \left( 1 + \frac{X_{ll}}{X_{LB}} \right) &= \frac{\bar{v}_t - \bar{v}_b}{jX_{LB}} + \bar{I}_{Lo} \end{aligned}$$

Now  $\bar{v}_b = V_B(\sin \delta + j \cos \delta)$  and  $I_{ll} = I_{ld} + jI_{lq}$  with eqn. (2.2) and eqn. (2.5), separation of d-q components gives

$$I_{ld} = \frac{E_q' - V_B \cos \delta + mkX_{LB}I_{dc} \cos \psi}{X_D} \quad (2.6)$$

$$I_{lq} = \frac{V_B \sin \delta + mkX_{LB}I_{dc} \sin \psi}{X_Q} \quad (2.7)$$

Where  $X_D = X_{LB} + X_H + X_d'$  and  $X_Q = X_{LB} + X_H + X_Q$

Now, linearization of eqn. (2.6) gives

$$\Delta I_{ld} = i_{d1}\Delta\delta + i_{d3}\Delta E_q' + i_{d5}\Delta Idc + i_{d6}\Delta m \quad (2.8)$$

$$\text{Where } i_{d1} = \frac{V_B \sin \delta_o}{X_D}; i_{d3} = \frac{1}{X_D}; i_{d5} = \frac{km_o X_{LB} \cos \psi_o}{X_D}; i_{d6} = \frac{kX_{LB} I_{dco} \cos \psi_o}{X_D}$$

And, linearization of eqn. (2.7) gives

$$\Delta I_{lq} = i_{q1}\Delta\delta + i_{q5}\Delta Idc + i_{q6}\Delta m \quad (2.9)$$

$$\text{Where } i_{q1} = \frac{V_B \cos \delta_o}{X_Q}; i_{q5} = \frac{km_o X_{LB} \sin \psi_o}{X_Q}; i_{q6} = \frac{kX_{LB} I_{dco} \sin \psi_o}{X_Q}$$

Now, the state space model of the system has been developed by linearization of the four machine equations and one STATCOM equation.

Machine Equations [7]:

$$\bullet \frac{d\delta}{dt} = \omega_b \omega \quad \text{Where } \omega_b \text{ is the base speed.} \quad (2.10)$$

$$\bullet \frac{d\omega}{dt} = P_m - P_e - D(\omega - \omega_o) \frac{1}{M} \quad (2.11)$$

Where  $P_m$  is the mechanical (turbine) power and  $P_e$  is generated electrical power.

$D$  is the damping co-efficient.

$$\bullet \frac{dE_q'}{dt} = \frac{E_{fd} - E_l}{T_{do}'} \quad (2.12)$$

Where  $E_l = E_q' + (X_d - X_d')I_{ld}$

Exciter Equation [7]:

The following exciter model has been used as shown in Fig. 2.2.

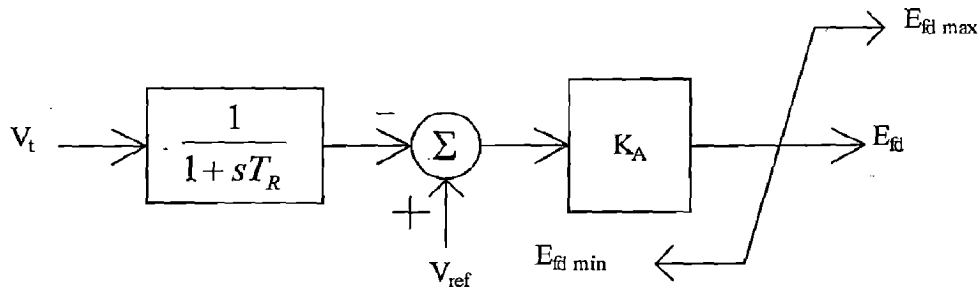


Figure 2.2: Exciter block diagram

$$\frac{dE_{fd}}{dt} = -\frac{1}{T_A} E_{fd} + \frac{K_A}{T_A} (V_{ref} - V_t) \quad (2.13)$$

▪ STATCOM Equation:

A state equation has been formulated by equating the real power feed to the STATCOM and the dc power absorbed. In other words, we can write it as,

$$P_{ac} = P_{dc} + \text{Losses in STATCOM circuit}$$

Since it has been assumed that, STATCOM is lossless, so losses are zero. Hence we have

$$P_{ac} = P_{dc}$$

$$\begin{aligned} \text{Now, } P_{ac} &= \text{Re}(V_L I_{Lo}^*) \\ &= V_{Ld} I_{Lod} + V_{Lq} I_{Loq} \end{aligned}$$

$$\begin{aligned} \text{And, } P_{dc} &= V_{dc} I_{dc} \\ &= L_{dc} \frac{dI_{dc}}{dt} I_{dc} \end{aligned}$$

$$\text{So, } L_{dc} I_{dc} \frac{dI_{dc}}{dt} = V_{Ld} I_{Lod} + V_{Lq} I_{Loq}$$

Putting the values of  $I_{Lod}$  and  $I_{Loq}$  from eqn. (2.5) and (2.6), we get

$$L_{dc} I_{dc} \frac{dI_{dc}}{dt} = c V_{Ld} I_{dc} \cos \psi + c V_{Lq} I_{dc} \sin \psi$$

$$\text{Or, } \frac{dI_{dc}}{dt} = \frac{mk}{L_{dc}} (V_{Ld} \cos \psi + V_{Lq} \sin \psi) \quad (2.14)$$

Now, linearization of eqn. (2.10) gives

$$\Delta \delta = \omega_b \Delta \omega \quad (2.15)$$

To linearize eqn. (2.11), we need the expression of power  $P_e$

Now,

$$\begin{aligned} P_e &= \text{Re}(\bar{V}_t \bar{I}_t^*) \\ &= E_q' I_{tlq} + (X_q - X_d') I_{tlq} I_{tld} \end{aligned} \quad (2.16)$$

So,

$$\begin{aligned} \Delta P_e &= \Delta E_q' I_{tlq0} + (X_q - X_d') I_{tlq0} \Delta I_{tld} + \{E_q' + (X_q - X_d') I_{tld0}\} \Delta I_{tlq} \\ &= K_{21} \Delta \delta + K_{23} \Delta E_q' + K_{25} \Delta I_{dc} + H_2 \Delta m \end{aligned} \quad (2.17)$$

Where,  $F_1 = (X_q - X_d')I_{tlqo}$ ;  $F_2 = E_{qo}' + (X_q - X_d')I_{tldo}$ ;  $K_{21} = F_1i_{d1} + F_2i_{q1}$   
 $K_{23} = F_1i_{d3} + I_{tlqo}'$ ;  $K_{25} = F_1i_{d5} + F_2i_{q5}$ ;  $H_2 = F_1i_{d6} + F_2i_{q6}$

Now, linearization of eqn. (2.11) gives

$$\begin{aligned}\Delta\omega &= (-\Delta P_e - D\Delta\omega)\frac{1}{M} \\ &= -\frac{K_{21}}{M}\Delta\delta - \frac{D}{M}\Delta\omega - \frac{K_{23}}{M}\Delta E_q' - \frac{K_{25}}{M}\Delta I_{dc} - \frac{H_2}{M}\Delta m\end{aligned}\quad (2.18)$$

Now, linearization of  $E_I$  equation gives

$$\begin{aligned}\Delta E_I &= \Delta E_q' + (X_d - X_d')\Delta I_{tld} \\ &= \Delta E_q' + (X_d - X_d')(i_{d1}\Delta\delta + i_{d3}\Delta E_q' + i_{d5}\Delta I_{dc} + i_{d6}\Delta m) \\ &= K_{31}\Delta\delta + K_{33}\Delta E_q' + K_{35}\Delta I_{dc} + H_3\Delta m\end{aligned}\quad (2.19)$$

Where

$$\begin{aligned}K_{31} &= (X_d - X_d')i_{d1}; K_{33} = 1 + (X_d - X_d')i_{d3} \\ K_{35} &= (X_d - X_d')i_{d1}; H_3 = (X_d - X_d')i_{d6}\end{aligned}$$

So, linearization of eqn. (2.12) gives

$$\begin{aligned}\frac{d\Delta E_q'}{dt} &= \frac{\Delta E_{fd} - \Delta E_I}{T_{do}'} \\ &= -\frac{K_{31}}{T_{do}'}\Delta\delta - \frac{K_{33}}{T_{do}'}\Delta E_q' + \frac{1}{T_{do}'}\Delta E_{fd} - \frac{K_{35}}{T_{do}'}\Delta I_{dc} - \frac{H_3}{T_{do}'}\Delta m\end{aligned}\quad (2.20)$$

From eqn. (2.5), we have

$$V_i^2 = (X_q I_{tlq})^2 + (E_q' - X_d' I_{tld})^2$$

This gives

$$\Delta V_i = K_{41}\Delta\delta + K_{43}\Delta E_q' + K_{45}\Delta I_{dc} + H_4\Delta m\quad (2.21)$$

Where

$$F = E_{qo}' - X_d' I_{tldo}; K_{41} = \frac{1}{V_{io}}(X_q^2 i_{q1} I_{tlqo} - F X_d' i_{d1}); K_{43} = \frac{1}{V_{io}} F(1 - X_d' i_{d3})$$

$$K_{45} = \frac{1}{V_{io}}(X_q^2 i_{q5} I_{tlqo} - F X_d' i_{d5}); H_4 = \frac{1}{V_{io}}(X_q^2 i_{q6} I_{tlqo} - F X_d' i_{d6})$$

Now, linearization of eqn. (2.13) gives

$$\begin{aligned}
\frac{d\Delta E_{fd}}{dt} &= -\frac{1}{T_A} \Delta E_{fd} - \frac{K_A}{T_A} \Delta V_t \\
&= -\frac{K_A}{T_A} K_{41} \Delta \delta - \frac{K_A}{T_A} K_{43} \Delta E_q' - \frac{1}{T_A} \Delta E_{fd} - \frac{K_A}{T_A} K_{45} \Delta I_{dc} - \frac{K_A}{T_A} H_4 \Delta m
\end{aligned} \tag{2.22}$$

Linearization of eqn. (2.14) gives

$$\frac{d\Delta I_{dc}}{dt} = K_{51} \Delta \delta + K_{53} \Delta E_q' + K_{55} \Delta I_{dc} + H_5 \Delta m \tag{2.23}$$

Where

$$F_3 = \frac{K}{L_{dc}} (V_{Ldo} \cos \psi_o + V_{Lqo} \sin \psi_o)$$

$$K_{51} = \frac{m_o K}{L_{dc}} \{ \cos \psi_o (X_q + X_u) i_{q1} - \sin \psi_o (X_d' + X_u) i_{d1} \}$$

$$K_{53} = \frac{m_o K}{L_{dc}} \sin \psi_o \frac{X_{LB}}{X_D}$$

$$K_{55} = \frac{m_o K}{L_{dc}} \{ \cos \psi_o (X_q + X_u) i_{q5} - \sin \psi_o (X_d' + X_u) i_{d5} \}$$

$$H_5 = F_3 + \frac{m_o K}{L_{dc}} \{ \cos \psi_o (X_q + X_u) i_{q6} - \sin \psi_o (X_d' + X_u) i_{d6} \}$$

In short we can write;

$$\begin{bmatrix} \Delta \delta \\ \Delta \omega \\ \Delta E_q' \\ \Delta E_{fd} \\ \Delta I_{dc} \end{bmatrix} = \begin{bmatrix} 0 & \omega_b & 0 & 0 & 0 \\ -\frac{K_{21}}{M} & -\frac{D}{M} & -\frac{K_{23}}{M} & 0 & -\frac{K_{25}}{M} \\ -\frac{K_{31}}{T_{do}'} & 0 & -\frac{K_{33}}{T_{do}'} & \frac{1}{T_{do}'} & -\frac{K_{35}}{T_{do}'} \\ -\frac{K_A}{T_A} K_{41} & 0 & -\frac{K_A}{T_A} K_{43} & \frac{1}{T_A} & -\frac{K_A}{T_A} K_{45} \\ K_{51} & 0 & K_{55} & 0 & K_{55} \end{bmatrix} \begin{bmatrix} \Delta \delta \\ \Delta \omega \\ \Delta E_q' \\ \Delta E_{fd} \\ \Delta I_{dc} \end{bmatrix} + \begin{bmatrix} 0 \\ -\frac{H_2}{M} \\ -\frac{H_3}{T_{do}'} \\ -\frac{K_A}{T_A} H_4 \\ H_5 \end{bmatrix} [\Delta m]$$

(2.24)

$$A = \begin{bmatrix} 0 & \omega_b & 0 & 0 & 0 \\ -\frac{K_{21}}{M} & -\frac{D}{M} & -\frac{K_{23}}{M} & 0 & -\frac{K_{25}}{M} \\ -\frac{K_{31}}{T_{do}'} & 0 & -\frac{K_{33}}{T_{do}'} & \frac{1}{T_{do}'} & -\frac{K_{35}}{T_{do}'} \\ -\frac{K_A}{T_A} K_{41} & 0 & -\frac{K_A}{T_A} K_{43} & \frac{1}{T_A} & -\frac{K_A}{T_A} K_{45} \\ K_{51} & 0 & K_{55} & 0 & K_{55} \end{bmatrix}$$

$$B = \begin{bmatrix} 0 & -\frac{H_2}{M} & -\frac{H_3}{T_{do}'} & -\frac{K_A}{T_A} H_4 & H_5 \end{bmatrix}^T$$

## 2.2 DERIVATION AND LINEARIZATION OF OUTPUT EQUATIONS

If the bus to which the STATCOM is connected, is considered, it can be observed there might be six output candidates

- Line current from bus 2 to bus 3
- Line current from bus 3 to bus 1
- Real power flow  $P_1$  and reactive power flow  $Q_1$  from bus 2 to bus 3
- Real power flow  $P_2$  and reactive power flow  $Q_2$  from bus 3 to bus 1

In this section, the six linearized output equations have been formulated.

I. Line current from bus 2 to bus 3 ( $\bar{I}_{tl}$ ) :

We can write  $I_{tl}^2 = I_{tld}^2 + I_{tlq}^2$  So,

$$\begin{aligned} \Delta I_{tl} &= \frac{1}{I_{tlo}} (I_{tldo} \Delta I_{tld} + I_{tlqo} \Delta I_{tlq}) \\ &= C_{11} \Delta \delta + C_{13} \Delta E_q' + C_{15} \Delta I_{dc} + D_1 \Delta m \end{aligned} \quad (2.25)$$

Where

$$\begin{aligned} C_{11} &= \frac{I_{tldo} i_{d1} + I_{tlqo} I_{q1}}{I_{tlo}}; C_{12} = \frac{I_{tldo} i_{d3}}{I_{tlo}} \\ C_{15} &= \frac{I_{tldo} i_{d5} + I_{tlqo} I_{q5}}{I_{tlo}}; D_1 = \frac{I_{tldo} i_{d6} + I_{tlqo} I_{q6}}{I_{tlo}} \end{aligned}$$

II. Line current from bus 3 to bus 1 ( $\bar{I}_{LB}$ ) :

Similarly  $\bar{I}_{LB} = \bar{I}_{tl} - \bar{I}_{Lo}$

$$= (I_{tld} + jI_{tlq}) - mkI_{dc} (\cos \psi + j \sin \psi)$$

$$\begin{aligned}
I_{LBd} &= I_{ild} - mkI_{dc} \cos \psi \\
\therefore \Delta I_{LBd} &= i_{d1} \Delta \delta + i_{d3} \Delta E_q' + (i_{d5} - km_o \cos \psi) \Delta I_{dc} + (i_{d6} - kI_{dco} \cos \psi) \Delta m \\
I_{LBq} &= I_{ilq} - mkI_{dc} \sin \psi \\
\therefore \Delta I_{LBq} &= i_{q1} \Delta \delta + (i_{q5} - km_o \sin \psi) \Delta I_{dc} + (i_{q6} - kI_{dco} \sin \psi) \Delta m
\end{aligned}$$

Now, we can write

$$\begin{aligned}
I_{LB}^2 &= I_{Lbd}^2 + I_{Lbq}^2 \\
\Delta I_{LB} &= \frac{1}{I_{LB0}} (I_{LBdo} \Delta I_{LBd} + I_{LBqo} \Delta I_{LBq}) \\
&= C_{21} \Delta \delta + C_{23} \Delta E_q' + C_{25} \Delta I_{dc} + D_2 \Delta m
\end{aligned} \tag{2.26}$$

Where

$$\begin{aligned}
C_{21} &= \frac{I_{LBdo} I_{d1} + I_{LBqo} i_{q1}}{I_{LB0}}; C_{23} = \frac{I_{LBdo}}{I_{LB0}} i_{d3} \\
C_{25} &= \frac{I_{LBdo} (i_{d5} - km_o \cos \psi) + I_{LBqo} (i_{q5} - km_o \sin \psi)}{I_{LB0}} \\
D_2 &= \frac{I_{LBdo} (i_{d6} - kI_{dco} \cos \psi) + I_{LBqo} (i_{q6} - kI_{dco} \sin \psi)}{I_{LB0}}
\end{aligned}$$

### III. Real power flow $P_1$ from bus 2 to bus 3 ( $P_1$ ):

We know  $P_1 = \text{Re}(\bar{V}_L \bar{I}_U^*)$

$$\begin{aligned}
&= \text{Re}((\bar{V}_t - jX_{tl} \bar{I}_U) \bar{I}_U^*) \\
&= I_{tlq} E_q' - (X_d' - X_q) I_{tlq} I_{ild} \\
\Delta P_1 &= C_{31} \Delta \delta + C_{33} \Delta E_q' + C_{35} \Delta I_{dc} + D_3 \Delta m
\end{aligned} \tag{2.27}$$

Where

$$C_{31} = K_{31}; C_{33} = K_{33}; C_{35} = K_{35}; D_3 = K_3$$

### IV. Reactive power flow $Q_1$ from bus 2 to bus 3 ( $Q_1$ ):

$$\begin{aligned}
Q_1 &= \text{Im}(\bar{V}_L \bar{I}_U^*) \\
&= \text{Im}((\bar{V}_t - jX_{tl} \bar{I}_U) \bar{I}_U^*) \\
&= I_{ild} E_q' - (X_d' + X_{tl}) I_{ild}^2 - (X_q + X_{tl}) I_{ilq}^2
\end{aligned}$$

Hence upon linearization we get

$$\Delta Q_1 = C_{41} \Delta \delta + C_{43} \Delta E_q' + C_{45} \Delta I_{dc} + D_4 \Delta m \tag{2.28}$$

Where

$$\begin{aligned}
F_4 &= E_{qo}' - 2(X_d' + X_{tl})I_{ldo} \\
F_5 &= -2(X_q + X_{tl})I_{lqo}; C_{41} = F_4 i_{d1} + F_5 i_{q1} \\
C_{43} &= F_4 i_{d3} + I_{ldo}; C_{45} = F_4 i_{d5} + F_5 i_{q5}; D_4 = F_4 i_{d6} + F_5 i_{q6}
\end{aligned}$$

V. Real power flow  $P_2$  from bus 3 to bus 1 ( $P_2$ ):

$$\begin{aligned}
\text{From Fig 2.1 } P_2 &= \text{Re}(\bar{V}_L \bar{I}_{LB}^*) \\
&= \text{Re}((\bar{V}_B + jX_{LB} \bar{I}_{LB}) \bar{I}_{LB}^*) \\
&= V_B I_{LBd} \sin \delta + V_B I_{LBq} \cos \delta
\end{aligned}$$

Linearization of above equation provides

$$\Delta P_2 = C_{51} \Delta \delta + C_{53} \Delta E_q' + C_{55} \Delta I_{dc} + D_5 \Delta m \quad (2.29)$$

Where

$$\begin{aligned}
C_{51} &= V_B (i_{d1} \sin \delta_o + i_{q1} \cos \delta_o) + V_B (I_{LBdo} \cos \delta_o - I_{LBqo} \sin \delta_o) \\
C_{53} &= V_B i_{d3} \sin \delta_o \\
C_{55} &= V_B \sin \delta_o (i_{d5} - km_o \cos \psi) + V_B \cos \delta_o (i_{q5} - km_o \sin \psi) \\
D_5 &= V_B \sin \delta_o (i_{d6} - kI_{dco} \cos \psi) + V_B \cos \delta_o (i_{q6} - kI_{dco} \sin \psi)
\end{aligned}$$

VI. Reactive power flow  $Q_2$  from bus 3 to bus 1 ( $Q_2$ ):

$$\begin{aligned}
\text{Similarly } Q_2 &= \text{Im}(\bar{V}_L \bar{I}_{LB}^*) \\
&= \text{Im}((\bar{V}_B + jX_{LB} \bar{I}_{LB}) \bar{I}_{LB}^*) \\
&= -V_B I_{LBq} \sin \delta + V_B I_{LBd} \cos \delta + X_{LB} I_{LB}^2
\end{aligned}$$

Linearization of above equation provides

$$\Delta Q_2 = C_{61} \Delta \delta + C_{63} \Delta E_q' + C_{65} \Delta I_{dc} + D_6 \Delta m \quad (2.30)$$

Where

$$\begin{aligned}
C_{61} &= V_B (i_{d1} \cos \delta_o - i_{q1} \sin \delta_o - I_{LBqo} \cos \delta_o - I_{LBdo} \sin \delta_o) + 2X_{LB} C_{21} \\
C_{63} &= V_B i_{d3} \cos \delta_o + 2X_{LB} C_{23} \\
C_{65} &= V_B [-\sin \delta_o (i_{q5} - km_o \sin \psi) + \cos \delta_o (i_{d5} - km_o \cos \psi)] \\
&\quad + 2X_{LB} C_{25} \\
D_6 &= V_B [-\sin \delta_o (i_{q6} - kI_{dco} \sin \psi) + \cos \delta_o (i_{d6} - kI_{dco} \cos \psi)] \\
&\quad + 2X_{LB} D_2
\end{aligned}$$

Now the output equations can be written in compact form as



$$\Delta y_1 = \Delta I_u = C_1 \Delta x + D_1 \Delta u$$

$$\Delta y_2 = \Delta I_{LB} = C_2 \Delta x + D_2 \Delta u$$

$$\Delta y_3 = \Delta P_1 = C_3 \Delta x + D_3 \Delta u$$

$$\Delta y_4 = \Delta Q_1 = C_4 \Delta x + D_4 \Delta u$$

$$\Delta y_5 = \Delta P_2 = C_5 \Delta x + D_5 \Delta u$$

$$\Delta y_6 = \Delta Q_2 = C_6 \Delta x + D_6 \Delta u$$

Where

$$C_1 = [C_{11} \quad 0 \quad C_{13} \quad 0 \quad C_{15}]$$

$$C_2 = [C_{21} \quad 0 \quad C_{23} \quad 0 \quad C_{25}]$$

$$C_3 = [C_{31} \quad 0 \quad C_{33} \quad 0 \quad C_{35}]$$

$$C_4 = [C_{41} \quad 0 \quad C_{43} \quad 0 \quad C_{45}]$$

$$C_5 = [C_{51} \quad 0 \quad C_{53} \quad 0 \quad C_{55}]$$

$$C_6 = [C_{61} \quad 0 \quad C_{63} \quad 0 \quad C_{65}]$$

And

$$\Delta x = [\Delta \delta \quad \Delta \omega \quad \Delta E_q' \quad \Delta E_{fd} \quad \Delta I_{dc}]^T$$

$$\Delta u = \Delta m$$

## CHAPTER 3

---

### CONTROLLER DESIGN AND VERIFICATION

In this chapter, a state-feedback controller has been designed. Important requirements of a control system may be outlined as:

- Most of the working systems are designed to be stable
- The output of the plant should approximate to its desired value within a prescribed tolerance.
- The system should be reasonably insensitive to the parameter variation.
- The system should be reasonably immune to the effects of noises.
- Its structure should be as simple as possible.

#### 3.1 CONCEPT OF STATE-FEEDBACK CONTROLLER [8], [9]:

State-feedback control law which has been used for this CSI STATCOM problem is given as:

$$\Delta u = -h\Delta x \quad (3.1)$$

Where  $\Delta u$  is the input of the system which is dependent upon the change in the state values.

$h$  is an arbitrary row matrix(1xn) and  $\Delta x$  is the state column matrix(nx1).

$$\text{We are having } \Delta x = A\Delta x + B\Delta u. \quad (3.2)$$

So, now the controlled system can be represented by

$$\Delta x = (A - Bh)\Delta x \quad (3.3)$$

#### 3.2 POLE PLACEMENT BY STATE FEEDBACK [8]:

Since the co-efficients  $h$  were arbitrarily chosen real numbers, the co-efficients of the characteristic polynomial of  $(A - Bh)$  can be given any desired values i.e., the closed loop poles can be located to arbitrary locations (subject to conjugate pairing).

One of the theorems of control system states that there exists a transformation matrix  $P$ , which converts the eq. (3.2) in the form given below, provide the system is controllable:

$$\Delta \bar{x} = \bar{A}\Delta \bar{x} + \bar{B}\Delta u$$

Where  $\Delta \bar{x} = P\Delta x$

$$\bar{A} = PAP^{-1} = \begin{bmatrix} 0 & 1 & 0 & \dots & 0 & 0 \\ 0 & 0 & 1 & \dots & 0 & 0 \\ \cdot & \cdot & \cdot & \dots & \cdot & \cdot \\ 0 & 0 & 0 & \dots & 0 & 1 \\ -\alpha_n & -\alpha_{n-1} & -\alpha_{n-2} & \dots & -\alpha_2 & -\alpha_1 \end{bmatrix}$$

Here, the numbers  $\alpha_n$  are the coefficients of the characteristic polynomial i.e.

$$|sI - A| = s^n + \alpha_1 s^{n-1} + \dots + \alpha_n s + \alpha_n$$

Similarly, eq. (3.3) can be transformed as

$$\Delta \bar{x} = (\bar{A} - \bar{B}\bar{h})\Delta \bar{x}$$

$$= \begin{bmatrix} 0 & 1 & 0 & \dots & 0 & 0 \\ 0 & 0 & 1 & \dots & 0 & 0 \\ \cdot & \cdot & \cdot & \dots & \cdot & \cdot \\ 0 & 0 & 0 & \dots & 0 & 1 \\ -\alpha_n - \bar{h}_1 & -\alpha_{n-1} - \bar{h}_2 & -\alpha_{n-2} - \bar{h}_3 & \dots & -\alpha_2 - \bar{h}_{n-1} & -\alpha_1 - \bar{h}_n \end{bmatrix} \Delta \bar{x}$$

And  $\bar{h} = hP^{-1}$

So, after proper pole placement, we got the characteristic equation of the above closed loop system as

$$s^n + \bar{\alpha}_1 s^{n-1} + \dots + \bar{\alpha}_n s + \bar{\alpha}_n$$

Hence,  $-\bar{\alpha}_n = -\alpha_n - \bar{h}_1$

Similarly, equating all members we get

$$\bar{h} = \begin{bmatrix} \bar{\alpha}_n - \alpha_n & \bar{\alpha}_{n-1} - \alpha_{n-1} & \dots & \bar{\alpha}_2 - \alpha_2 & \bar{\alpha}_1 - \alpha_1 \end{bmatrix} \quad (3.4)$$

And  $h = \bar{h}P \quad (3.5)$

### 3.3 CONTROL STRATEGY FOR THE CSI STATCOM DAMPING CONTROLLER:

There are two parameters which can be used for controlling the active or reactive power from the STATCOM. These are

- i. Phase angle  $\psi$  which is the phase difference between the modulating signal and carrier signal. It is also the phase angle of the STATCOM current. As stated earlier, to damp out the rotor oscillations reactive power exchange is only necessary. So, angle between the bus voltage and injected current should be fixed  $90^\circ$  or  $-90^\circ$ . That's why we shall not use the phase angle  $\psi$  as input signal.
- ii. Modulation index  $m$  is the best candidate since by changing it, magnitude of reactive power changes accordingly.

### 3.4 MATLAB COMMAND FOR POLE PLACEMENT:

$K = \text{PLACE}(A, B, P)$  computes a state-feedback matrix  $K$  such that the eigen values of  $A-BK$  are those specified in vector  $P$ . No eigen value should have a multiplicity greater than the number of inputs.

### 3.5 CALCULATION OF CONTROLLER GAIN MATRIX:

The open loop system has the following eigen values:

$$-0.41 + 107.18i$$

$$-0.41 - 107.18i$$

$$-98.56$$

$$-1.75$$

$$-0.00461$$

By using the state feedback controller  $\Delta m = -h\Delta x$  we can place the closed loop poles at the locations where system response is the best. Unfortunately, there is not any specific method which will provide those optimized poles. So, the only option is hit and trial method. One of the possible combinations of poles that was used:

$$-0.4509 + 117.897i$$

$$-0.4509 - 117.897i$$

-108.418  
-1.930  
-0.00507

Accordingly, the gain matrix  $h$  was calculated and given as:

$$h = [-1.367 \quad -0.0979 \quad -4.910 \quad -0.1396 \quad -0.3976]$$

### 3.6 OBSERVER DESIGN [8]:

For, the state feedback control we need all the states, out of which only the  $I_{dc}$  is locally available, while all other states are need to be communicated to the controller via a wired or a wireless link. This adds not only huge capital cost but also errors which could cause the controller to collapse. So, an *observer* should be used which anticipates the instantaneous value of the states from the output signal.

The dynamic equation of the Luenberger observer is given by

$$\hat{x}(t) = A\hat{x}(t) + Bu(t) - L\{y(t) - \hat{y}(t)\} \quad (3.6)$$

Where  $\hat{\phantom{x}}$  indicates that it is the estimated value of that quantity.

We know, if the system is observable, its states can be estimated with a  $n$ -dimensional observer of the form

$$\hat{x}(t) = (A + LC)\hat{x}(t) + Bu(t) - Ly(t)$$

Again this time, arbitrarily chosen the eigen values can be used and corresponding value of matrix  $L$  can be calculated by the same MATLAB command, *place*.

#### 3.6.1 PROCEDURE OF SELECTION OF STABILIZING OUTPUT SIGNAL FOR STATCOM [10]

The procedure to select stabilizing signals for supplementary controller of the STATCOM using the RHP-zeros and the HSV can be described as follows:

**Step 1)** After placing the STATCOM, we choose the stabilizing signal candidates for supplementary control.

**Step 2)** For each candidate, we calculate the RHP-zeros. If any RHP-zeros is encountered then the corresponding candidate should be discarded.

By considering different inputs-outputs for any plant different zeros will appear. Those inputs-outputs, which produce the RHP zeros are undesirable because of the limiting performance of the closed loop.

Considering the negative feedback system with plant  $G = z/p$  and a constant gain controller  $K = k$ , the closed-loop transfer function is

$$G_c = \frac{KG}{1+KG} = \frac{kz}{p+kz} = k \frac{z_{cl}}{p_{cl}}$$

From the above closed-loop transfer function, it is obvious that the locations of zeros are unchanged, while pole locations are changed by the feedback. As the feedback gain decreases, the closed-loop poles will be moved to open-loop poles and as the feedback gain increases, the closed-loop poles will be moved from open-loop poles to open-loop zeros, which may lead to gain instability.

**Step 3)** We check the observability and controllability of the remaining candidates using the Hankel Singular Values (HSV). The candidate with the largest HSV is more preferred, which shows that the corresponding signal is more responsive to the mode of oscillation and is the final choice.

Controllability and observability of a system play an important role in selecting input-output signals. In order to specify which combination of input-output contains more information about the system internal states, one possible approach is to evaluate observability and controllability indexes of the system. A linear time invariant system can be defined as

$$G: \begin{cases} \dot{x} = Ax + Bu \\ y = Cx + Du \end{cases}$$

Two possible ways to check that the above system is controllable are

- (A,B) is controllable if and only if matrix  $\Phi$  has full rank, where n is the number of states.,

$$\phi = [B \quad AB \quad A^2B \quad \dots \quad A^{n-1}B]$$

- (A,B) is controllable if and only if the controllability Gramian matrix defined as

$$P = \int_0^{\infty} e^{At} BB^T e^{A^T t} dt$$

is positive definite, which has full rank  $n$ . Matrix  $P$  is the solution to the following Lyapunov equation:

$$AP + PA^T + BB^T = 0$$

Also, there are two possible ways to check the observability of the above system

- $(A,C)$  is controllable if and only if matrix  $\psi$  has full rank, where  $n$  is the number of states.,

$$\psi = [C \quad CA \quad CA^2 \quad \dots \quad CA^{n-1}]^T$$

- $(A,C)$  is controllable if and only if the controllability Gramian matrix defined as

$$Q = \int_0^{\infty} e^{A^T t} C C^T e^{A t} dt$$

is positive definite, which has full rank  $n$ . Matrix  $Q$  is the solution to the following Lyapunov equation:

$$A^T Q + Q A + C C^T = 0$$

The Hankel Singular Values (HSV) are observability-controllability indices, defined as

$$\sigma_i = \sqrt{\lambda_i(PQ)}, \quad i=1, \dots, n$$

which reflects the joint controllability and observability of the states of a system where  $\lambda_i$  is the  $i^{\text{th}}$  eigenvalue of  $PQ$ .

### 3.6.2 CHOICE OF OUTPUT SIGNAL:

Table 3.1 gives the Hankel value as well as the number of RHP zeros for the all six selected out puts:

Table 3.1: Output signal selection parameters

Output signal	Hankel singular value	No. of RHP zeros
$I_H$	8.8564	1
$I_{LB}$	10.1163	1
$P_1$	6.8840	1
$Q_1$	2.1101	0
$P_2$	8.8873	2
$Q_2$	2.7068	1

So, it can be concluded that  $Q_1$  is the only candidate having no RHP zeros. Hence it was our output signal for state estimation.

We chose the observer pole at locations same as that of controller poles.

The corresponding gain matrix comes to be

$$L = [2.8 \quad 35.0 \quad -9.7 \quad 4631.4 \quad 0.6]$$

Now, estimated error

$$\begin{aligned} \tilde{x} &= x - \hat{x} = Ax + Bu - [A\hat{x} + Bu - L(y - \hat{y})] \\ &= A(x - \hat{x}) + L(Cx + Du - C\hat{x} + Du) \\ &= A(x - \hat{x}) + LC(x - \hat{x}) \\ &= (A + LC)\tilde{x} \end{aligned}$$

And

$$\begin{aligned} \dot{\tilde{x}} &= Ax + Bu - B\dot{\hat{x}} \\ &= Ax - Bh(x - \tilde{x}) \\ &= (A - Bh)x + Bh\tilde{x} \end{aligned}$$

The complete system matrix comprising controller as well as observer is given below.

$$\begin{bmatrix} \dot{x} \\ \dot{\tilde{x}} \\ x \end{bmatrix} = \begin{bmatrix} A - Bh & Bh \\ 0 & A + LC \end{bmatrix} \begin{bmatrix} x \\ \tilde{x} \end{bmatrix}$$



Some the eigen value of the above matrix comes with real positive part. With only controller and without observer we get very satisfactory results. So, the observer was dropped and the work moved ahead only with controller.

### 3.7 NON LINEAR SIMULATIONS:

#### 3.7.1 INITIAL VALUE CALCULATION:

In appendix A-2, values initial values of all quantities such as line voltages (magnitude and angle), line currents have been listed. These have been calculated by Gauss-Siedel load flow technique.

Some other quantities were calculated as;

- $\delta_o$ :  $\delta_o = \text{angle}(V_1 \angle \theta + jX_q \bar{I}_d)$
- $\psi_o$ : It can be calculated by using the following phasor diagram

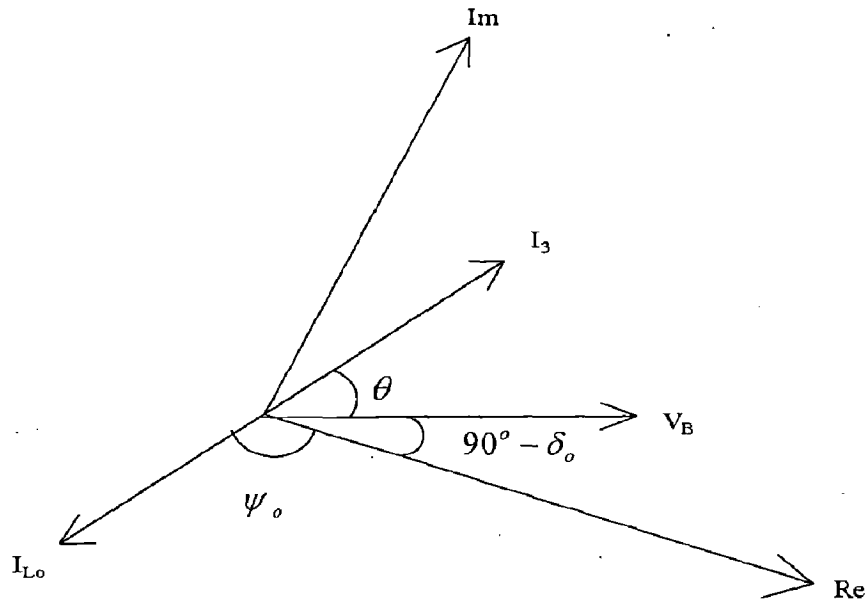


Figure 3.1: Phasor dia. of system

We can see,  $I_3$  is injected current at bus 3 according to the convention of load flows. Also  $V_B$  was taken as the reference direction, but all derivation was carried out taking the real axis ( $R_e$ ) as reference direction. So, it is necessary to convert all the quantities according to this new reference direction. Now,  $\psi_o$  which is the angle of current  $I_{L0}$  is given as:

$$\psi_o = -[\pi - (90^\circ - \delta_o + \theta)]$$

- $m_o$  and  $I_{dco}$ : Eq (2.1) gives  $|I_{Lo}| = m_o k I_{dco}$ . So, if we keep  $m_o = 0.5$  then  $I_{dco}$  can also be calculated.

### 3.7.2 DIFFERENTIAL AND ALGEBRAIC EQUATIONS:

At first, it is assumed that system is running normally in steady state. A three phase short circuit takes place at the generator terminal and it was cleared after 0.1 second. To observe the system transient behavior, it is needed to solve the following differential equations:

$$\frac{d\delta}{dt} = \omega_b \omega$$

$$\frac{d\omega}{dt} = P_m - P_e - D(\omega - \omega_o) \frac{1}{M}$$

$$\frac{dE_q'}{dt} = \frac{E_{fd} - E_q'}{T_{do}'}$$

$$\frac{dE_{fd}}{dt} = -\frac{1}{T_A} E_{fd} + \frac{K_A}{T_A} (V_{ref} - V_t)$$

$$\frac{dI_{dc}}{dt} = \frac{mk}{L_{dc}} (V_{Ld} \cos \psi + V_{Lq} \sin \psi)$$

Algebraic equations are:

$$I_{ud} = \frac{E_q' - V_B \cos \delta + mk X_{LB} I_{dc} \cos \psi}{X_D}$$

$$I_{uq} = \frac{V_B \sin \delta + mk X_{LB} I_{dc} \sin \psi}{X_Q}$$

$$\bar{E}_t = \bar{E}_q' + j(X_d - X_d') I_{ud}$$

$$I_{LOd} = c I_{dc} \cos \psi$$

$$I_{LOq} = c I_{dc} \sin \psi$$

Only the first four equations are required for the uncompensated system. These equations have been solved using fourth order Runge-Kutta method.

### 3.7.3 PLOTS:

We can compare the transient response of the compensated and the uncompensated system for  $P_e = 1.0 pu$  which are shown below:

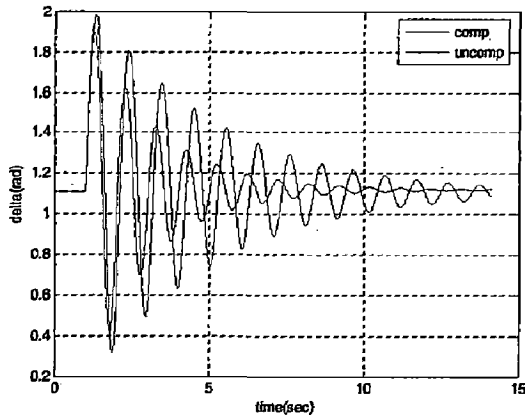


Figure 3.2: Rotor angle oscillation

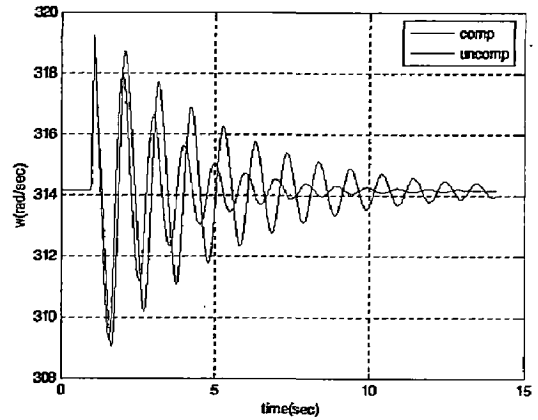


Figure 3.3: Rotor speed oscillation

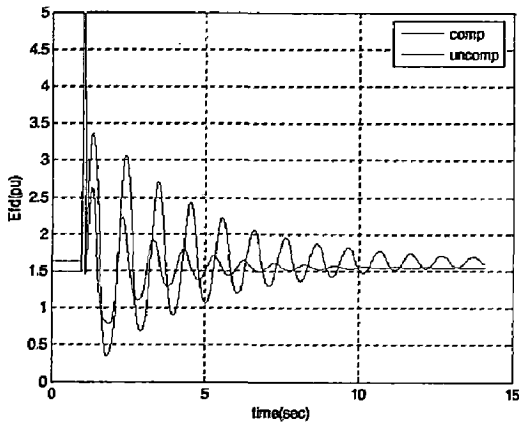


Figure 3.4: Variation of  $E_q'$

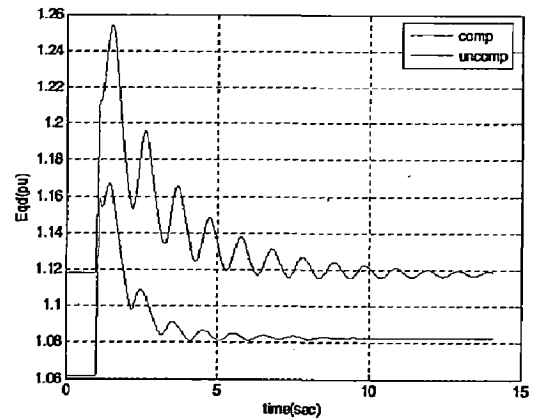


Figure 3.5: Variation of  $E_{fd}$

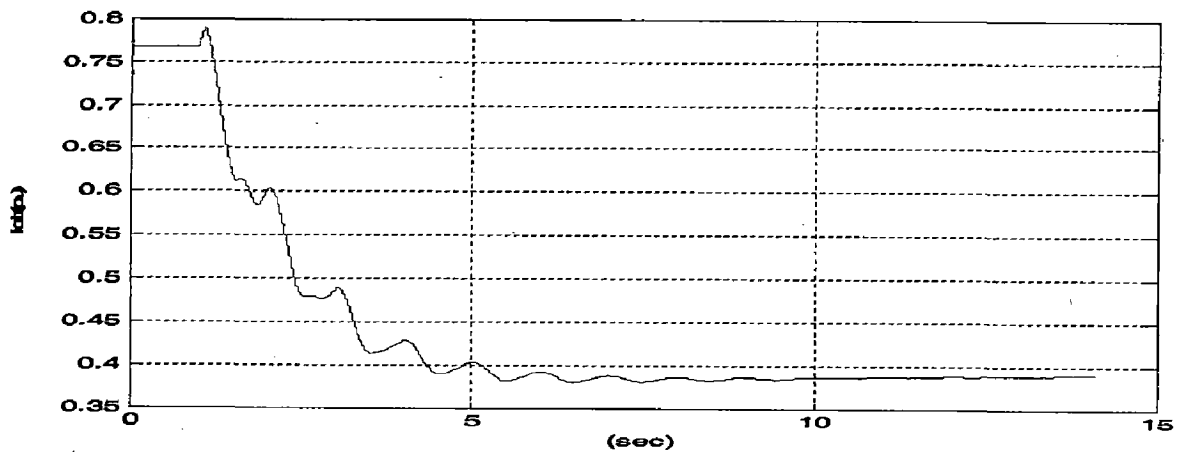


Figure 3.6: Variation of  $I_{dc}$

But if we run the simulation for  $P_e = 1.1 \text{ pu}$ , we found that the uncompensated system is unstable while the compensated system recovers nicely.

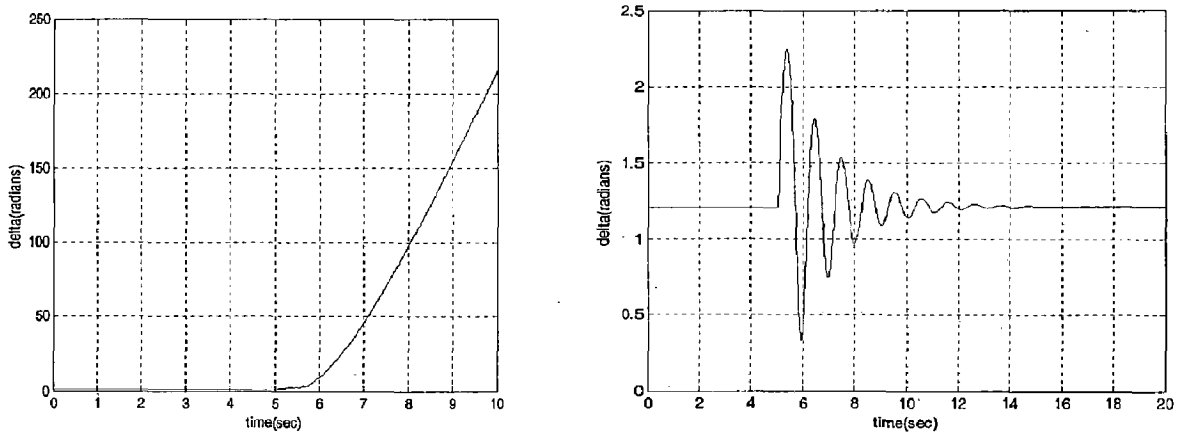


Figure 3.7: Comparison of system stability for  $P_e = 1.1 \text{ pu}$

### 3.8 DISCUSSION ON RESULTS:

Figure 3.2 shows the rotor angle oscillations of the uncompensated as well as compensated system. The overshoot of rotor oscillation for uncompensated and compensated system is 2.0 and 1.9 radians respectively. So, the stability margin is 0.1 radian i.e. 5.73 degrees. Also, we can see that the angle oscillation of the uncompensated system persists for more than 15 sec. while, for the compensated system it almost vanishes after 9 sec. In, other words, we can say that the damping controller has effectively improved the transient response of the system. Same type of damping effect we can observe on other quantities: angular speed,  $E_q'$ ,  $E_{fd}$  and  $I_{dc}$ .

## CHAPTER 4

### CSI STATCOM IMPLEMENTATION IN PSCAD

In the previous chapters an ideal STATCOM was considered, in which the losses and the inverter harmonics were neglected. However, in practice, there is no electrical system without losses as well as no inverter without harmonics. Therefore, in this chapter, a practical CSI STATCOM will be studied through detail digital simulation using PSCAD/EMTDC.

#### 4.1 BASIC CONFIGURATION OF A CURRENT SOURCE INVERTER:

Basically a CSI inverter is a bridge circuit of GTOs with anti parallel connected diodes. A current source is needed at its dc side as shown in the Fig 4.1. To filter out higher order harmonics, a star connected capacitor bank is connected to its output side.

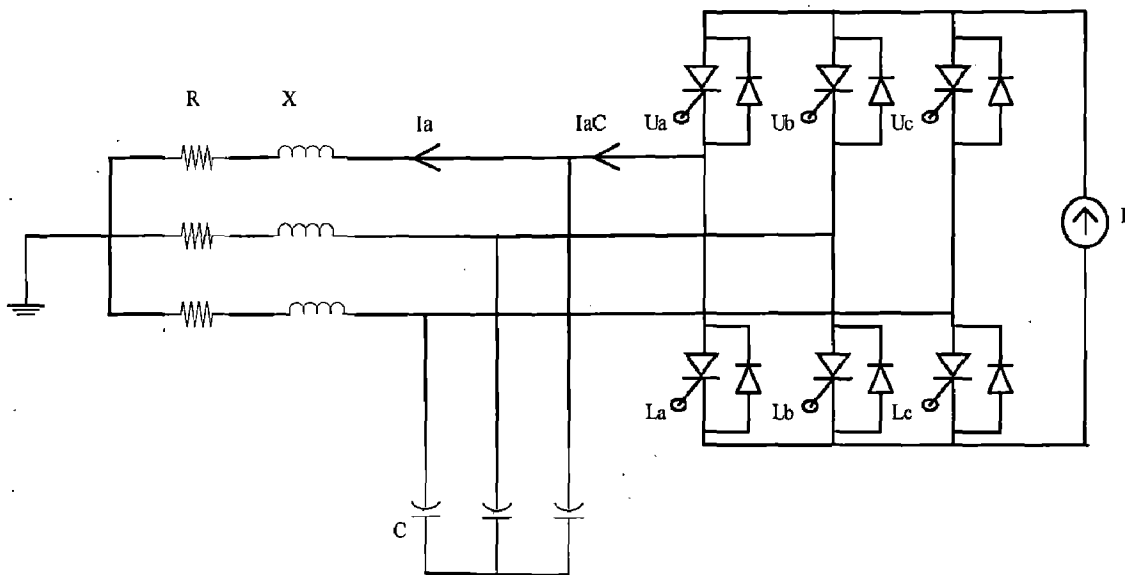


Figure 4.1: Circuit diagram of current source inverter

#### 4.2 SWITCHING SCHEME FOR THE INVERTER [11]:

For switching the trilogic pulse width modulation scheme has been used.

#### 4.2.1 PRACTICAL IMPLEMENTATION & THE TRAJECTORY TAKEN BY THE TRI-LOGIC PWM:

In this scheme, for generating the switching pulses, three sinusoidal modulating signals  $S_{m1}$ ,  $S_{m2}$  and  $S_{m3}$  (corresponding to phases a, b and respectively) are compared to a carrier signal  $S_c$ .

$$S_{m1} = \sin(\omega t + \phi) \quad (4.1)$$

$$S_{m2} = \sin(\omega t - 120^\circ + \phi) \quad (4.2)$$

$$S_{m3} = \sin(\omega t + 120^\circ + \phi) \quad (4.3)$$

And subsequently, the signals  $X_j$  ( $j=1, 2, 3$ ) are generated according to:

If  $S_{mj} > S_c$ ; then  $X_j = +1$

& if  $S_{mj} < S_c$ ; then  $X_j = -1$

In general it can be said, when the triangular pulses go higher than modulating sinusoidal signals ( $S_{mj}$ ),  $X_j$  are assigned -1 otherwise they are made +1.

#### 4.2.2 TRANSLATION OF $X_j$ TO $Y_j$ :

The formula for translating the bi-logic PWM variables  $X_j(t)$  to tri-logic variable  $Y_j(t)$  is based on the linear mapping:

$$\begin{bmatrix} Y_a(t) \\ Y_b(t) \\ Y_c(t) \end{bmatrix} = \frac{1}{2} [C] \begin{bmatrix} X_1(t) \\ X_2(t) \\ X_3(t) \end{bmatrix} \quad (4.4)$$

$$\text{Where } [C] = \begin{bmatrix} 1 & -1 & 0 \\ 0 & 1 & -1 \\ -1 & 0 & 1 \end{bmatrix}$$

So, 
$$Y_a(t) = \frac{X_1(t) - X_2(t)}{2} \quad (4.5)$$

$$Y_b(t) = \frac{X_2(t) - X_3(t)}{2} \quad (4.6)$$

$$Y_c(t) = \frac{X_3(t) - X_1(t)}{2} \quad (4.7)$$

Hence  $Y_j(t)$  can have one of the 3 values: **+1, 0 or -1.**

In, table 4.1 given below; the transformation from bi-logic to tri-logic signal is given in detail:

Table 4.1: Truth table of translations from bi-logic to tri-logic signal

BI-LOGIC			TRI-LOGIC			STATE
$X_1$	$X_2$	$X_3$	$Y_a$	$Y_b$	$Y_c$	DESIGNATION
+1	+1	+1	0	0	0	#D, #E, #F
+1	+1	-1	0	+1	-1	#1
+1	-1	+1	+1	-1	0	#2
+1	-1	-1	+1	0	-1	#3
-1	+1	+1	-1	0	+1	#4
-1	+1	-1	-1	+1	0	#5
-1	-1	+1	0	-1	+1	#6
-1	-1	-1	0	0	0	#D, #E, #F

#### 4.2.3 INTERPRETATION OF VALUE OF $Y_j(t)$ :

As shown in the Fig 4.1, in Inverter Bridge there are 3-valves in upper group –  $U_a$ ,  $U_b$  &  $U_c$  and 3-valves in lower group:  $L_a$ ,  $L_b$  &  $L_c$ .

If  $Y_j = +1$  ; then the upper valve of phase j is ON & lower valve is OFF

If  $Y_j = -1$  ; then the lower valve of phase j is ON & upper valve is OFF

If  $Y_j = 0$ ; then both valves are OFF.

In table 4.2 all the  $2^3$  combinations for  $Y_j$  are listed.

Table 4.2: Current source converter states

TRI-LOGIC			UPPER VALVE			LOWER VALVE			STATE
$Y_a$	$Y_b$	$Y_c$	$U_a$	$U_b$	$U_c$	$L_a$	$L_b$	$L_c$	DESIGNATION
0	+1	-1		1				1	#1
+1	-1	0	1				1		#2
+1	0	-1	1					1	#3
-1	0	+1			1	1			#4
-1	+1	0		1		1			#5
0	-1	+1			1		1		#6
0	0	0	1			1			#D, #0
				1			1		#E, #0
					1			1	#F, #0

Following can be observed from the above table:

- All the states are assigned a particular identification like #1, #2... #E, #F.
- In the first 6 states, values of  $Y_j$  are unique. So, we can predict which valves are conducting & which are not.
- For the last 3 states, values of  $Y_j$  is (0, 0, 0). In these states, the upper & the lower valves of the same phase are 'ON'. So, the ac currents in the lines are zero.

Now, two trilogic states are called "contiguous" when the transition from one to the other can be carried out by a single switching action. The "single switching action" consists of turning OFF one of the two valves that has been ON and turning ON the new valve to form the next state.

For example tri-logic state #2 or (+1, -1, 0) is shown in Fig 5.3. There can be 4 single switching actions.

1. Keep  $L_b$  unchanged and switch OFF valve  $U_a$ . There are two possible switchings: Switch ON either  $U_b$  or  $U_c$ . So, contiguous states are (0, 0, 0) & (0, -1, +1) i.e. states #E & #6 respectively.



2. Now keep  $U_a$  unchanged & switch OFF valve  $L_b$ . Then either  $L_a$  or  $L_c$  can be switched ON. So, contiguous states are  $(0, 0, 0)$  &  $(+1, 0, -1)$  i.e. states #D & #3 respectively. This process is shown pictorially as below:

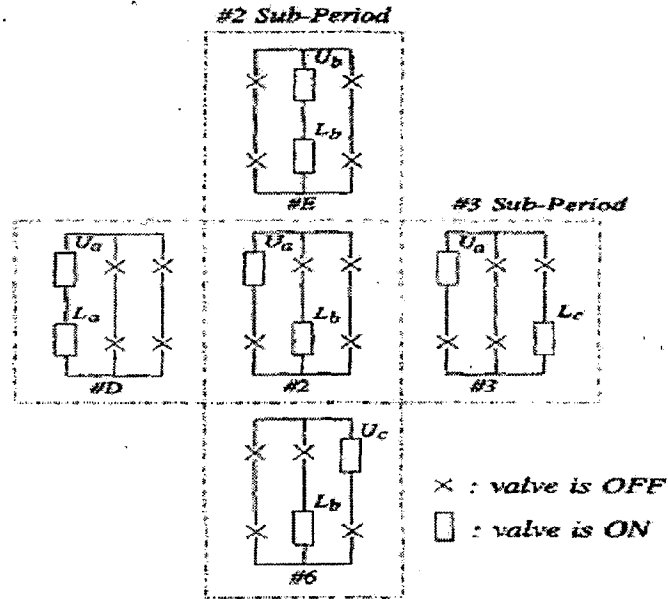


Figure 4.2: Single switching actions & contiguous states of state #2

#### 4.2.4 CONTIGUOUS STATE NETWORK:

By examining the contiguity of all the states in Table 4.2, it is found that they form a network as shown in Fig. 4.3.

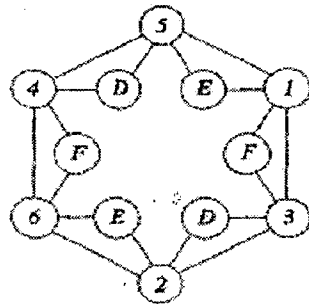


Figure 4.3: Contiguous states of 6-valve current source converter

#### 4.2.5 SIMULATION STUDY

In this work the frequency of the triangular pulses has been taken as 21 times that of the sinusoidal modulating signal. It means that there are 21 triangles per period of sinusoidal

modulating signal. The modulation index has been kept 0.8. Then we run the simulation & get the  $Y_j$  waveforms which is shown in Fig 4.4.

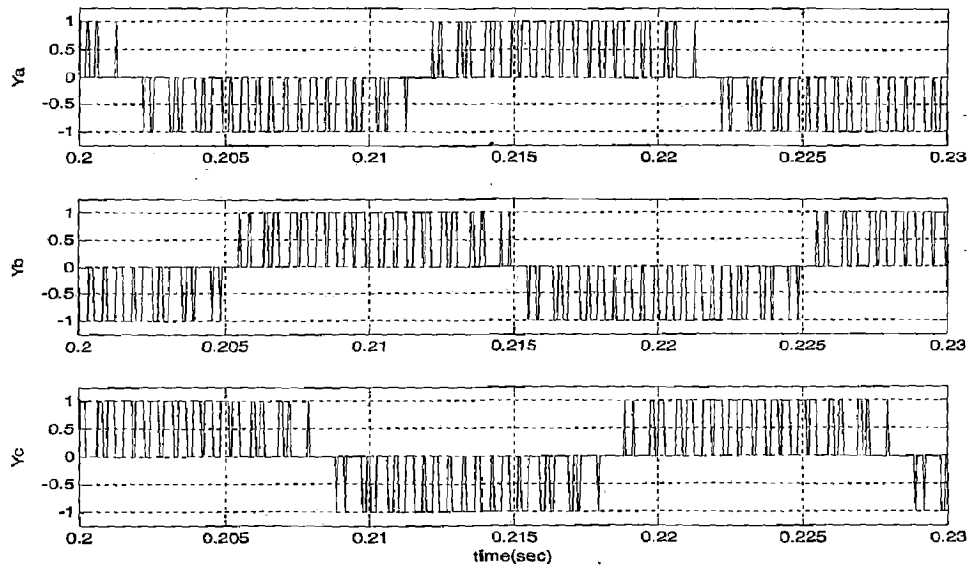


Figure 4.4:  $Y_j$  waveforms

After identifying the possible existing states, we get total 6 sub periods as given in Table 4.3

Table 4.3: Sequence of tri logic states

SEQUENCE IN SUBPERIOD	SUB PERIOD IDENTIFICATION	CONTIGUITY INTERPRETATION (0)
202606202606202606202606202	#2	E
303202303202303202303202303	#3	D
101303101303101303101303101	#1	F
505101505101505101505101505	#5	E
404505404505404505404505404	#4	D
606404606404606404606404606	#6	F

Now, following points can be observed from the Table 4.3:

1. Each sub period consist of oscillating transitions involving 3 trilogic states.
2. Two of the 3 states are uniquely specified i.e. whether it is #2 or #6 & so on.

3. One of the states is '0' (0, 0, 0) which creates ambiguity.

Now, mentioned earlier, the state '0' can correspond to any of the states #D, #E or #F. The appropriate choice of the states (#D, #E or #F) is done by following the Fig 4.4. In this figure, for example, it is observed that the state #E is contiguous with the state 2 and 6. Therefore, the state '0' in the first row of the Table 4.3 should be realized by state #E. Simultaneously, following the Fig 4.4 for fifth row of the Table 4.3, the '0' state should be represented by the state #D. In the same manner, the appropriate states for representing the '0' state for other sub-periods have also been determined and are shown in Table 4.3.

#### **4.2.6 TRANSITION BETWEEN SUB PERIODS:**

The transition between sub-periods occurs when the state passes from the last member of one line to the first member of the next line. As Table 4.3 is examined with the network of contiguous States of Fig. 4.2, one can see that the transitions: #2 to #3, #3 to #1, #1 to #5. . . are all contiguous transitions.

#### **4.2.7 DESIGNING THE GATING SEQUENCE OF VALVES:**

The design of gating sequence of valves is based on the features embodied in Table 4.3 & Fig. 4.4. Each of the six sub periods has two nonzero state members forming a group. The group consists of the first member of the current sub period and first member of the previous sub-period. From Table 4.3, these are (#2, #6), (#3, #2), (#1, #3). . . for the first, second, third sub-periods respectively and so on. By checking whether the input ( $Y_a(t)$ ,  $Y_b(t)$ ,  $Y_c(t)$ ) has group membership or not, the Gating Logic can identify the arrival of a nongroup, nonzero state and therefore the beginning of a new sub period. The new sub period forms a new nonzero group membership for the identification of the next sub period. The #0 or (0, 0, 0) state in each sub period is based on a look-up table from the last column in Table 4.3

Now, for suppressing the higher order harmonics, a filter is needed at the CSI STATCOM terminals. For this purpose a passive filter in the star connected form of a 330  $\mu$ F capacitor is used at the terminals of the STATCOM.

### 4.3 SIMULATION OF CURRENT SOURCE INVERTER:

For this simulation, a special switching scheme is needed which was described in this chapter in full detail. A component called '*TLG\_SWITCHING*' was designed which generates the required signals for the block '*Interpolated Firing Pulses*'.

INPUT: The three tri-logic signals Y1, Y2, Y3

PARAMETERS: By double clicking over it, a window opens, showing 6 parameters called 'SUBPERIOD'. Each of these 6 parameters needs following inputs:

- I. ENTER THE FIRST ELEMENT OF THE GROUP
- II. ENTER THE SECOND ELEMENT OF THE GROUP
- III. ENTER THE CONTIGUOUS STATE

OUTPUT: There are six outputs, upper three is given to the block '*Interpolated Firing Pulses*' of the upper GTOs connected to phases A, B and C respectively. Lower three is given to the block '*Interpolated Firing Pulses*' of the lower GTOs connected to phases A, B and C respectively. Output is either 1 or 0. Whenever output becomes 1, it means that particular GTO is on and vice-versa.

#### 4.3.1 PROGRAMMING LOGIC:

The programming logic of the block is described by the following flow chart:

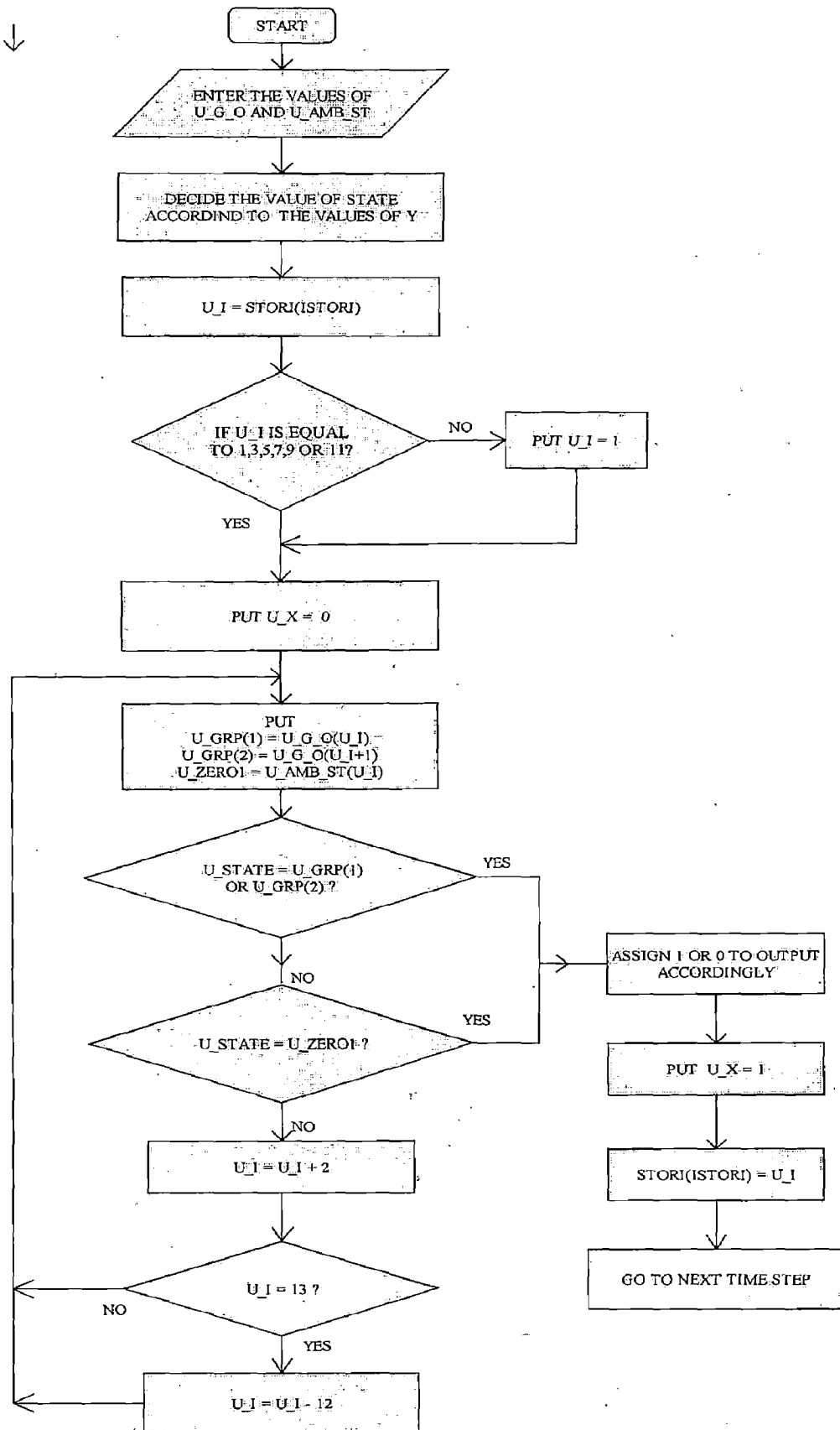


Figure 4.5: Flow chart for programming logic of component 'TLG\_SWITCHING'

### 4.3.2 CIRCUIT PARAMETERS:

Circuit Parameters Values:

Load resistance  $R = 5 \text{ ohm}$

Load inductance  $X = 0.1 \text{ H}$

Filter capacitor  $C = 330 \text{ }\mu\text{F}$

Current source  $I = 10 \text{ amp}$

Frequency of sinusoidal modulating signal = 50 Hz

Frequency of triangular wave = 1050 Hz

Modulation index = 0.8

### 4.3.3 OUTPUT WAVEFORMS:

The output wave forms of the current in phase A before and after the filter is shown in the Fig 4.7 and Fig 4.8 respectively.

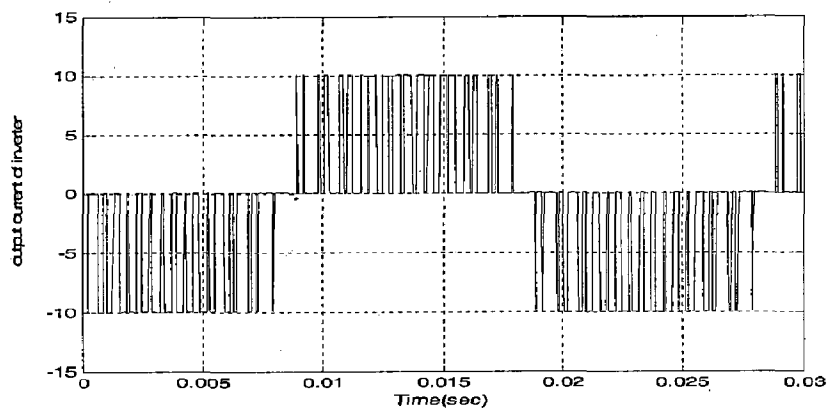


Figure 4.6: Current waveform before the filter in phase A

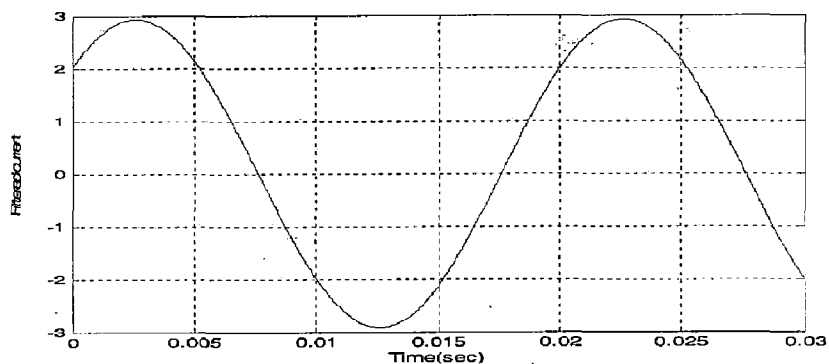


Figure 4.7: Current waveform after the filter in phase A

#### 4.4 CASE STUDY:

Fig 4.9 shows the single line diagram of the system studied in this work. The star connected capacitor bank provides a low impedance path to higher order components and vice-versa. Fig 4.10 shows the controller used.

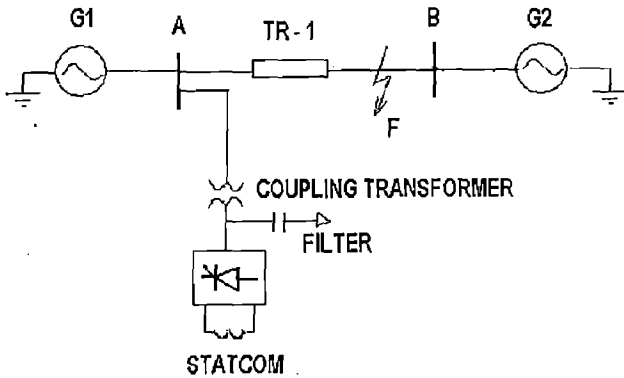


Figure 4.8: Compensated power system

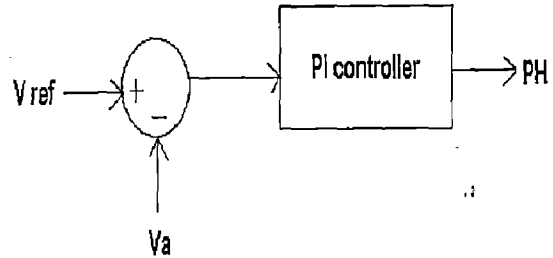


Figure 4.9: Phase angle control strategy

Here 'PH' stands for  $\phi$  given in eqn. (4.1), (4.2) and (4.3)

Proportional gain  $K_p = -100$

Integral gain  $K_I = -0.0001 \text{ sec}$

#### A. RESULTS: VARIATION OF REFERENCE VOLTAGE:

To check the workability of our STATCOM, at first we set the reference voltage to 0.95 pu, then it is changed to 1.0 pu and finally it is set back to 0.95 pu. Fig 4.10 shows, the bus voltage of the Bus A follows the reference voltage very nicely. Fig 4.11 shows the reactive power exchange which gives the explanation how it could be done.

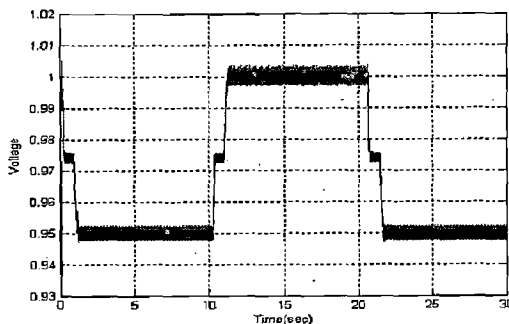


Figure 4.10: Variation of bus voltage

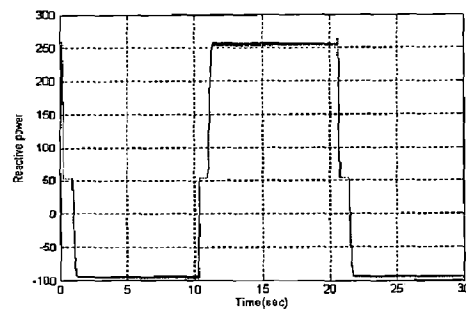


Figure 4.11: Variation of bus reactive power

## B. RESULTS: EFFECTIVENESS DURING FAULT:

Next coming plot will show the voltage profile of bus A voltage for the most severe fault, for both cases compensated as well as uncompensated systems.

Three phase to ground fault:

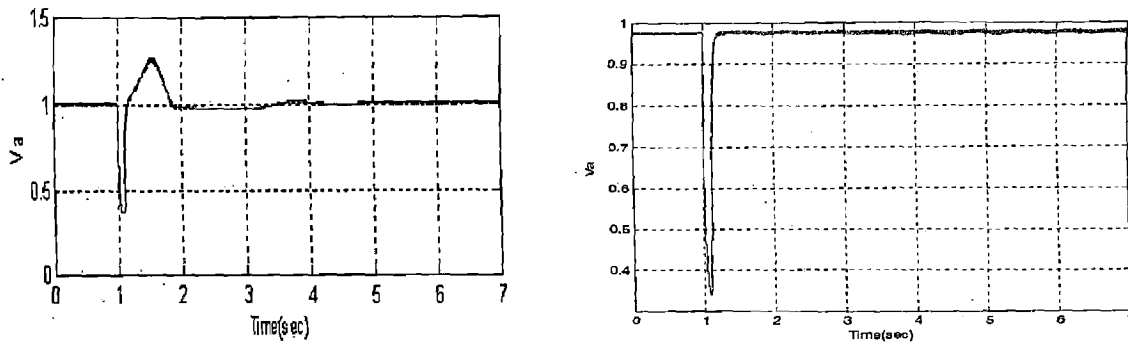


Figure 4.12: Voltage profile for A-B-C-G fault (comp. and uncomp.)

### 4.5 ACTIVE FILTER:

Then the same STATCOM was tried with a larger system (27 bus system) [11], it was found that the whole control system collapsed, i.e. it could not able to raise the bus voltage to the required level. It was due to the permanently connected capacitor bank, which creates control problems for bigger systems since capacitor bank is continuously supplying the reactive power. Also, it could not filter out the higher order harmonics in a satisfactory manner. So, another option is the application of an active filter. Its circuit diagram is shown below:

Ⓜ



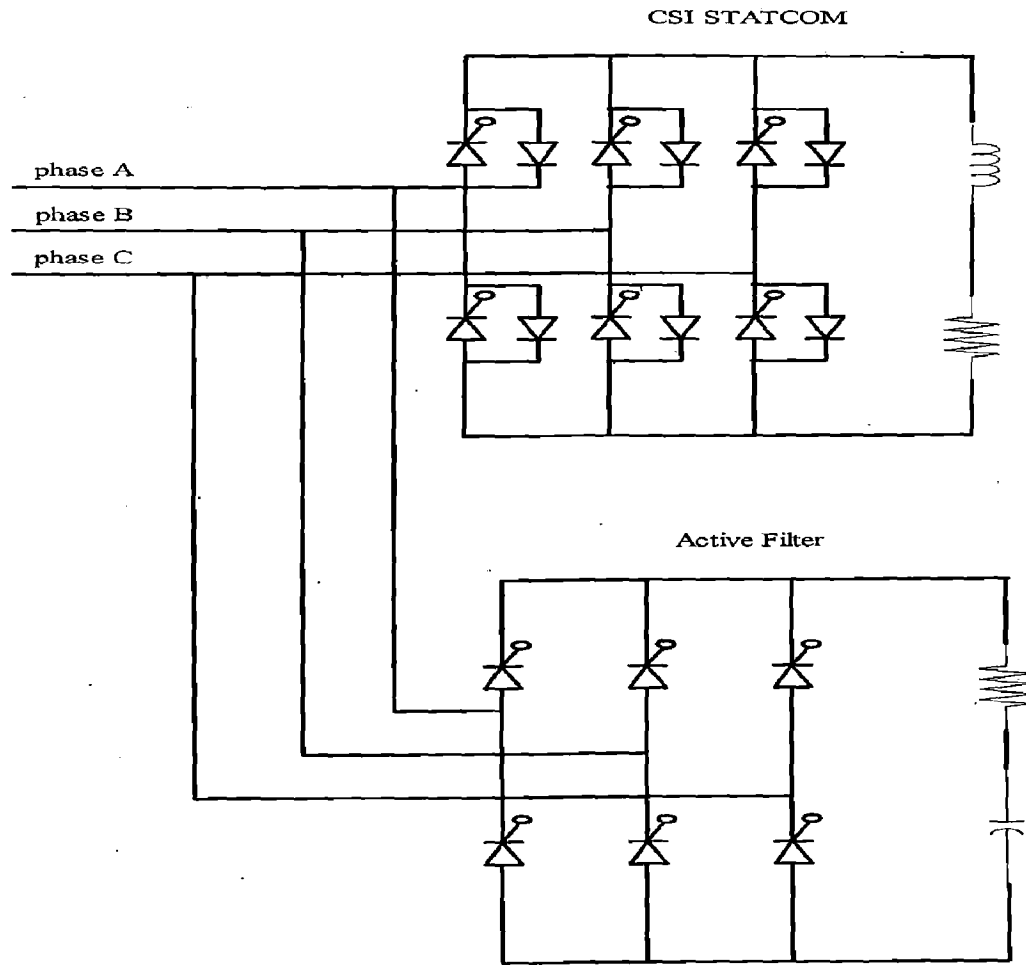


Figure 4.13: Circuit diagram of active filter

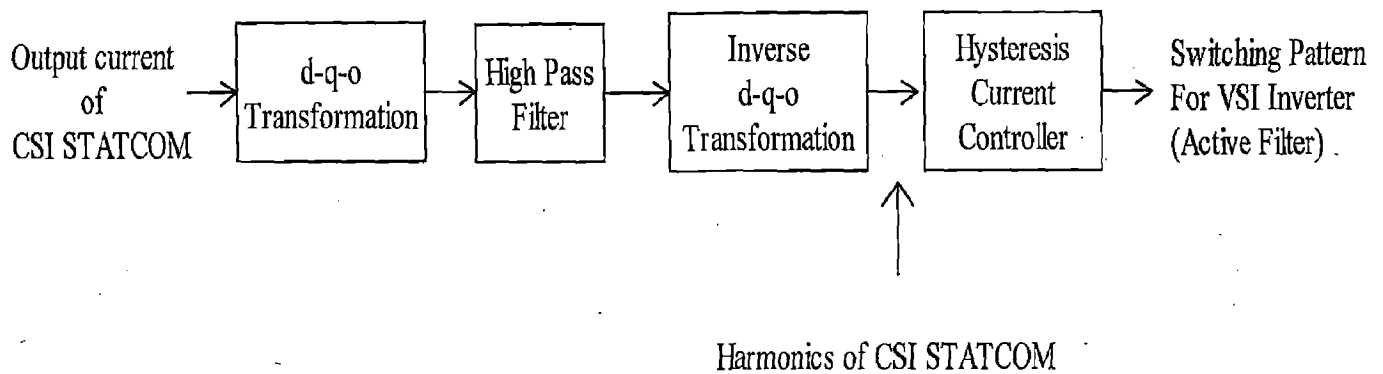


Figure 4.14: Functional block diagram of active filter

**4.5.1 d-q-o TRANSFORMATION [7]:**

The transformation from the abc phase variables to d-q-o variables can be written in the following matrix form:

$$\begin{bmatrix} i_d \\ i_q \\ i_o \end{bmatrix} = \frac{2}{3} \begin{bmatrix} \cos \theta & \cos(\theta - 2\pi/3) & \cos(\theta + 2\pi/3) \\ \sin \theta & \sin(\theta - 2\pi/3) & \sin(\theta + 2\pi/3) \\ 1/2 & 1/2 & 1/2 \end{bmatrix} \begin{bmatrix} i_a \\ i_b \\ i_c \end{bmatrix}$$

And the inverse transformation is given as

$$\begin{bmatrix} i_a \\ i_b \\ i_c \end{bmatrix} = \begin{bmatrix} \cos \theta & -\sin \theta & 1 \\ \cos(\theta - 2\pi/3) & -\sin(\theta - 2\pi/3) & 1 \\ \cos(\theta + 2\pi/3) & -\sin(\theta + 2\pi/3) & 1 \end{bmatrix} \begin{bmatrix} i_d \\ i_q \\ i_o \end{bmatrix}$$

We know the combined mmf wave due to the currents in the three armature phases travel along the periphery of the stator at synchronous velocity  $\omega_s$ . This is also the velocity of the rotor. Therefore, for balanced synchronous operation, the armature mmf appears stationary with respect to the rotor and has a sinusoidal space distribution. Now we can resolve this armature mmf into two sinusoidally distributed mmf waves stationary with respect to the rotor, so that one has its peak over the d-direction and other over the q-direction. Therefore  $i_d$  may be interpreted as the instantaneous current in a fictitious armature winding which rotates at the same speed as the rotor, and remains in such a position that its axis always coincides with the d-axis. A similar interpretation applies to  $i_q$  except that it acts on the q-axis.

For balanced steady-state conditions, the phase currents may be written as follows:

$$\begin{aligned} i_a &= I_m \sin(\omega_s t + \phi) \\ i_b &= I_m \sin(\omega_s t + \phi - \frac{2\pi}{3}) \\ i_c &= I_m \sin(\omega_s t + \phi + \frac{2\pi}{3}) \end{aligned}$$

Using dqo transformation:

$$\begin{aligned} i_d &= I_m \sin(\omega_s t + \phi - \theta) \\ i_q &= -I_m \cos(\omega_s t + \phi - \theta) \\ i_o &= 0 \end{aligned}$$

For synchronous operation, the rotor speed  $\omega_r$  is equal to the angular frequency  $\omega_s$  of the stator currents. Hence,

$$\theta = \omega_s t = \omega_r t$$

Therefore

$$i_d = I_m \sin \phi$$

$$i_q = -I_m \sin \phi$$

In other words, balanced alternating phase currents in the abc reference frame appears as direct currents in the d-q-o reference frame.

#### 4.5.2 HIGH PASS FILTER:

The high pass filter as its name suggests allows to pass only the frequencies above the characteristic frequency. The transfer function is given as

$$Y(t) = L^{-1} \left\{ \frac{G \left( \frac{s}{\omega_c} \right)^2 X(s)}{1 + 2\zeta \left( \frac{s}{\omega_c} \right) + \left( \frac{s}{\omega_c} \right)^2} \right\}$$

G = Gain

$\omega$  = Characteristic frequency

$\zeta$  = Damping Ratio

s = Laplace operator

$L^{-1}$  = Inverse Laplace transform

The Damping Ratio  $\zeta$  determines the stability of the outputs, given by all nine functions above. The output is stable for positive damping, where as a negative damping constant will result in growing oscillations at the characteristic frequency  $\omega_c$ .

#### 4.5.3 HYSTERESIS CURRENT CONTROL [13]:

Hysteresis band current control is basically as instantaneous feedback current control method of PWM where the actual current continually tracks the reference current within a hysteresis band. Fig 4.16 explains the operation principle.

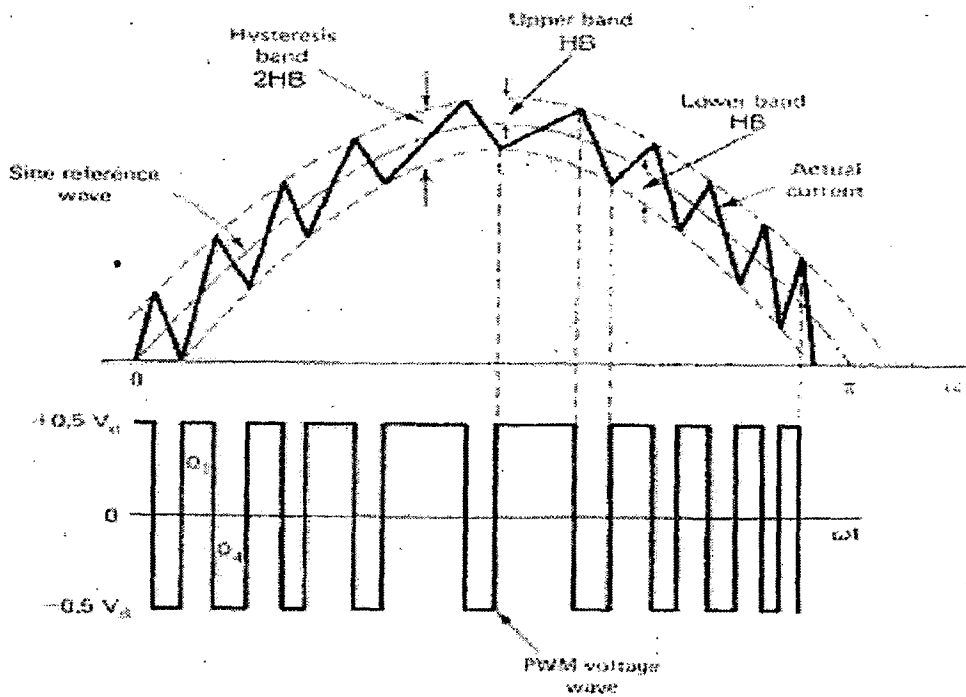


Figure 4.15: Principle of hysteresis band current control

As the current exceeds a prescribed hysteresis band, the upper switch in the bridge is turned off and the lower switch is turned on. As a result the current decays due to the transition of output voltage from  $+0.5V_d$  to  $-0.5V_d$ . As the current crosses the lower band limit, the lower switch is turned off and the upper switch is turned on. The actual current is forced to track the sine reference wave within the hysteresis band by back and forth switching of the upper and lower switches. The inverter then essentially becomes a current source with peak to peak current ripple, which is controlled within hysteresis band irrespective of voltage fluctuation.

#### 4.5.4 STRATEGY OF THE ACTIVE FILTER:

A VSI inverter, connected to same bus, actually serves the purpose of active filter. The current output of the CSI STATCOM was taken and converted into d-q-o components. As we know, if the three phase currents are completely symmetrical then d and q components are dc and o component is zero. But since the output currents are not completely sinusoidal, so these components are fluctuating around that dc component. Then these d, q and o components were pass through a high pass filter and then the inverse d-q-o transform was carried out, which finally gives the harmonic components of

the CSI STATCOM. Inverse of these currents were used as reference current for the hysteresis current control. This gives the switching sequence for the VSI inverter which generates almost same current waveform as this reference current which is actually the higher order harmonics of the CSI STATCOM. Finally this current is injected in the system where higher order harmonics are cancelled out and only sinusoidal current is injected in the system.

#### 4.5.5 RESULTS: EFFECTIVENESS OF ACTIVE FILTER:

To get the effectiveness of the active filter scheme a 27-bus system was simulated and the reference voltage of the bus to which the STATCOM is connected is kept 1.0 pu. It can be observed that in the Fig 4.17 that bus voltage acquires 1.0 pu but current waveform is not sinusoidal. So, right now it is not working properly and it needs some modification.

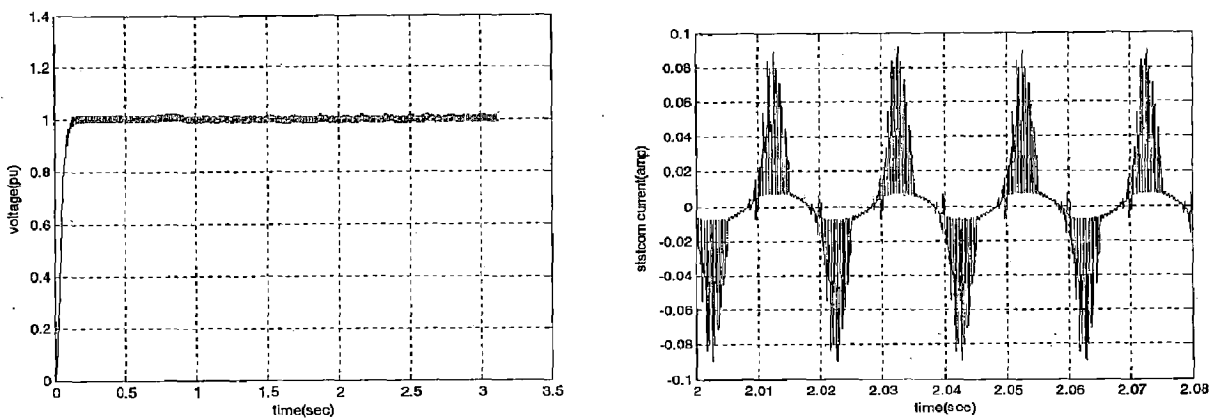


Figure 4.16: Voltage rise and current waveform

#### 4.6 DISCUSSION ON RESULTS:

1. If we look at the voltage plot of uncompensated system, we found that voltage at bus A is near about 0.975 pu. After connecting the STATCOM in the system we found that voltage becomes 1.0 pu. So, we can say the simulated STATCOM serves the required purpose of voltage boost.
2. Now we look at the voltage at bus A during different faults for compensated as well as uncompensated systems. It is given in Table 4.4.

Table 4.4: Voltages during the faults

	A-G	A-B	A-B-G	A-B-C-G
V <sub>a</sub> (uncompensated system)	0.75	0.66	0.548	0.337
V <sub>a</sub> (compensated system)	0.787	0.69	0.575	0.354

So, we see it provides a voltage support for power system and make the system performance better during short circuit faults.

In case of an active filter, we can see from the Fig 4.16 that injected current near the peaks gets a lot of spikes but rest of the part is almost sinusoidal. This suggests that if more work is done then we can get totally sinusoidal current.

## CONCLUSION AND SCOPE FOR FURTHER WORK

---

In summary, this thesis established the Phillips-Heffron model for single machine infinite bus. It demonstrated the stabilizing and damping effect of a state feedback controller. The transient behavior of the system can be effectively improved by using the CSI STATCOM with a damping controller.

The PSCAD/EMTDC simulation suggested that the CSI STATCOM with a passive filter raised the Bus voltage as required and it helped during the faults but only for the small systems.

So, an active filter was used for the same purpose for the 27 bus system but the current was not coming exactly sinusoidal especially near the peaks. So, more work is needed to design the filter to get the exactly sinusoidal currents.

The scope for further work is listed below:

- Design of an observer which can anticipate the states.
- Removal of peak spikes near the peak of injected current while using as active filter
- Modeling and analysis of the multi-machine power system installed with a CSI STATCOM

## REFERENCES

---

1. Laszlo Gyugyi, "Dynamic Compensation of AC Transmission Lines by Solid State Synchronous Voltage Sources", IEEE Transactions on Power Delivery, Vol. 9, No. 2, April 1994, pp: 904-911
2. N. G. Hingorani and L. Gyugyi, "Understanding FACTS: Concepts and Technology of Flexible AC Transmission Systems", New York: IEEE Press, 2000.
3. Yang Ye, Mehrdad Kazerani and Victor H. Quintana, "Current-Source Converter Based STATCOM: Modeling and Control", IEEE Transactions on Power Delivery, Vol. 20, no. 2, April 2005, pp: 795-800.
4. Mehrdad Kazerani and Yang Ye, "Comparative Evaluation of Three-Phase PWM Voltage- and Current-Source Converter Topologies in FACTS Applications", Power Engineering Society Summer Meeting, 2002, IEEE Publication, Date: 2002, Vol-1, pp: 473-479
5. B. M. Han & S. I. Moon, "Static Reactive-Power Compensator Using Soft-Switching Current-Source Inverter", IEEE Transactions on Industrial Electronics, Vol. 48, No. 6, December 2001.
6. H. F. Wang, "Phillip-Heffron model of power systems installed with STATCOM and applications", IEE Proc-Gener, Transm: Distrib., Vol. 146, No. 5, September 1999, pp: 521-527
7. P. Kundur, "Power System Stability and control", Electric Power Research Institute, McGraw-Hill, Inc. 1994
8. M. Gopal, "Modern Control System Theory", Wiley Eastern Limited, 1993
9. Dong Shen and P. W. Lehn "Modeling, Analysis, and Control of a Current Source Inverter--Based STATCOM", IEEE Transactions on Power Delivery, Vol. 17, no. 1, January 2002, pp: 248-252
10. M. M. Farsangi, Y. H. Song, and Y. Lee, "Choice of FACTS Devices Control Inputs for Damping Interarea Oscillations", IEEE Transactions on Power Systems, Vol. 19, no. 2, May 2004, pp: 1135-1143



11. Xiao Wang and Boon-Teck Ooi, "Unity PF Current-Source Rectifier Based on Dynamic Trilogic PWM". IEEE Transactions on Power Electronics, Vol. 8, no. 3, July 1993, pp: 288-294.
12. Biswarup Das and Bikash C. Pal, "Voltage Control Performance of AWS Connected For Grid Operation", IEEE Transactions on Energy Conversion, Vol. 21, no. 2, June 2006
13. Bimal K. Bose, "Modern Power Electronics and AC Drives", Pearson Education, Inc., 2004
14. Luis T. Moran, D. Ziogas and Geza Joos, "Analysis and Design of a Three-phase Current Source Solid-state Var Compensator", IEEE Transactions on Industry Applications, Vol. 25, no. 2, March/April 1989, pp: 356-365
15. H.F. Bilgin, M. Ermis, K.N. Kose, A. Cetin, I. Cadirci, A. Acik, A. Terciyanli, C. Kocak, and M. Yorukoglu, "Reactive power compensation of coal mining excavators using a new generation STATCOM", Industry Applications Conference 2005, 40<sup>th</sup> IAS Annual Meeting Conference record of the 2005, pp: 185-197
16. Bingsen Wang, "Shunt compensation using CSI based STATCOM", ECE714 Project Report, Department of Electrical and Computer Engineering, University of Wisconsin – Madison, Spring 2003

## APPENDIX-A

### A-1 SYSTEM PARAMETERS OF THE SYSTEM SHOWN IN Fig 2.1:

$H = 3.0s$ ,  $D = 0.015$ ,  $T_{do}' = 5.044s$ ,  $X_d = 1.0$ ,  $X_d' = 0.3$ ,  $X_q = 0.6$ ,  $X_{tl} = 0.3$   
 $X_{LB} = 0.3$ ,  $K_A = 10.0$ ,  $T_A = 0.01s$ ,  $T_C = 0.05s$ ,  $L_{dc} = 0.6H$

### A-2 GAUSS SIEDEL LOAD FLOW RESULT: All data are in pu.

BUS NO	VOLTAGE	ANGLE(DEGREE)	REAL POWER	REACTIVE POWER	CURRENT MAG	CURRENT ANGLE
1	1.0000	0.000000	-1.000000	0.153536	1.011718	-171.271198
2	1.0000	34.915206	1.000000	0.153536	1.011718	26.186405
3	1.0000	17.457603	0.000000	0.307072	0.307072	-72.542397

### A-3 HIGH PASS FILTER DATA:

Gain: 1.0  
 Damping ratio: 0.2  
 Characteristic frequency: 10 Hz

### A-4 SYSTEM PARAMETERS OF THE SYSTEM SHOWN IN Fig 4.8:

#### Generator data

	Rated voltage	Rated capacity	Phase angle	Impedance
G1	230 KV	100 MVA	0	$0.005 + j15.708$
G1	230 KV	100 MVA	30° Lag	$0.0025 + j7.854$

#### Transformer data:

	Voltage ratio	Rated capacity	Connection	Leakage reactance
Coupling Tranx	230/23 KV	100 MVA	Y-Y	0.1 pu

#### Transmission line data

	Equivalent parameters
TR - 1	$0.0025 + j7.854$

APPENDIX-B

MATLAB Program for non-linear simulation

B-1 MAIN

\*\*\*\*\*runge\_thss\*\*\*\*\*

```

pole_plcmt;
step=0.01;
XLB=0.3; Xtl=0.3; Xq=0.6; Xd=1.0; Xdd=0.3;
XD=XLB + Xtl + Xdd;
XQ=XLB + Xtl + Xq; kk=0.8; mmo=0.5; mm=mmo; c=mm*kk;
freq=50; D=0.015; Tdo=5.044; KA=10.0; TA=0.01; H=3.0; M=H/(pi*freq);
ILOo=abs(I(3)); Vto=abs(volt(2));
sio=(pi/2-delo+angle(I(3)))-pi; VB=1; Idco=ILOo/c;
Itlqo=(VB*sin(delo) + c*XLB*Idco*sin(sio))/XQ;
const1=VB*cos(delo) - c*XLB*Idco*cos(sio);
const2=sqrt(Vto^2 - (Xq*Itlqo)^2);
Itldo=(const2 - const1)/(XLB+Xtl);
Eqod=Itldo*Xdd + const2;
del=delo; wo=2*pi*50; w=wo; si=sio; Eqd=Eqod; Idc=Idco; Pm=1; t=0; Q_out=-Q(3);
Efd= Eqod + (Xd-Xdd)*Itldo; Efd=Efd; vref = Efd/KA + Vto;
tout=0.0; del_out=delo; w_out=wo; Eqd_out=Eqd; Efd_out=Efd; Idc_out=Idco; vt=1.0; mm_out=mmo;
Peo=Eqod*Itlqo + (Xq-Xdd)*Itlqo*Itldo;
P_out=Peo; V_out=voltmag(3);
%-----
for ii=0:step:1
    c=mm*kk;
    k1=step*fn_del(w);
    l1=step*fn_w(del,w,Eqd,Idc,1,sio,mm);
    m1=step*fn_Eqd(del,Eqd,Efd,Idc,1,sio,mm);
    n1=step*fn_Efd(del,Eqd,Efd,Idc,delo,sio,Idco,1,mm,vref);
    o1=step*fn_Idc(del,Eqd,Idc,1,sio,mm);
    k2=step*fn_del(w+0.5*l1);
    l2=step*fn_w(del+0.5*k1,w+0.5*l1,Eqd+0.5*m1,Idc+0.5*o1,1,sio,mm);
    m2=step*fn_Eqd(del+0.5*k1,Eqd+0.5*m1,Efd+0.5*n1,Idc+0.5*o1,1,sio,mm);
    n2=step*fn_Efd(del+0.5*k1,Eqd+0.5*m1,Efd+0.5*n1,Idc+0.5*o1,delo,sio,Idco,1,mm,vref);
    o2=step*fn_Idc(del+0.5*k1,Eqd+0.5*m1,Idc+0.5*o1,1,sio,mm);

    k3=step*fn_del(w+0.5*l2);
    l3=step*fn_w(del+0.5*k2,w+0.5*l2,Eqd+0.5*m2,Idc+0.5*o2,1,sio,mm);
    m3=step*fn_Eqd(del+0.5*k2,Eqd+0.5*m2,Efd+0.5*n2,Idc+0.5*o2,1,sio,mm);
    n3=step*fn_Efd(del+0.5*k2,Eqd+0.5*m2,Efd+0.5*n2,Idc+0.5*o2,delo,sio,Idco,1,mm,vref);
    o3=step*fn_Idc(del+0.5*k2,Eqd+0.5*m2,Idc+0.5*o2,1,sio,mm);

    k4=step*fn_del(w+l3);
    l4=step*fn_w(del+k3,w+l3,Eqd+m3,Idc+o3,1,sio,mm);
    m4=step*fn_Eqd(del+k3,Eqd+m3,Efd+n1,Idc+o3,1,sio,mm);
    n4=step*fn_Efd(del+k3,Eqd+m3,Efd+n3,Idc+o3,delo,sio,Idco,1,mm,vref);
    o4=step*fn_Idc(del+k3,Eqd+m3,Idc+o3,1,sio,mm);

    k=(k1+2*k2+2*k3+k4)/6;
    l=(l1+2*l2+2*l3+l4)/6;
    m=(m1+2*m2+2*m3+m4)/6;
    n=(n1+2*n2+2*n3+n4)/6;
    o=(o1+2*o2+2*o3+o4)/6;

```



```

    t=t+step;
    del=del+k;
    w=w+1;
    Eqd=Eqd+m;
    Efd=Efd+n;
    if(Efd>=5)
        Efd=5;
    end
    if(Efd<=-5)
        Efd=-5;
    end
    Idc=Idc+o;
    Itlq=(VB*sin(del)+mm*kk*XLB*Idc*sin(sio))/XQ;
    Itld=(Eqd-VB*cos(del)+mm*kk*XLB*Idc*cos(sio))/XD;
    Pe=Eqd*Itlq + (Xq-Xdd)*Itlq*Itld;
    Q=mm*kk*Idc*((Eqd-(Xdd+Xtl)*Itld)*cos(sio) - (Xq+Xtl)*Itlq*sin(sio));
    Q_out=[Q_out Q];

mm=-mat_K*[del-delo;w-wo;Eqd-Eqod;Efd-Efdo;Idc-Idco] + mmo;

if(mm>1)
    mm=1;
end
if(mm<-1)
    mm=-1;
end
%-----
tout = [tout t];
del_out = [del_out del];
w_out = [w_out w];
Eqd_out = [Eqd_out Eqd];
Efd_out = [Efd_out Efd];
Idc_out = [Idc_out Idc];
P_out = [P_out Pe];
mm_out = [mm_out mm];
volt_3=sqrt((Xq+Xtl)*Itlq*(Xq+Xtl)*Itlq + (Eqd-(Xdd+Xtl)*Itld)*(Eqod-(Xdd+Xtl)*Itld));
V_out=[V_out volt_3];
end
for ii=0:step:0.1
    c=mm*kk;
    k1=step*fn_del(w);
    l1=step*fn_w(del,w,Eqd,Idc,2,sio,mm);
    m1=step*fn_Eqd(del,Eqd,Efd,Idc,2,sio,mm);
    n1=step*fn_Efd(del,Eqd,Efd,Idc,delo,sio,Idco,2,mm,vref);
    o1=step*fn_Idc(del,Eqd,Idc,2,sio,mm);

    k2=step*fn_del(w+0.5*l1);
    l2=step*fn_w(del+0.5*k1,w+0.5*l1,Eqd+0.5*m1,Idc+0.5*o1,2,sio,mm);
    m2=step*fn_Eqd(del+0.5*k1,Eqd+0.5*m1,Efd+0.5*n1,Idc+0.5*o1,2,sio,mm);
    n2=step*fn_Efd(del+0.5*k1,Eqd+0.5*m1,Efd+0.5*n1,Idc+0.5*o1,delo,sio,Idco,2,mm,vref);
    o2=step*fn_Idc(del+0.5*k1,Eqd+0.5*m1,Idc+0.5*o1,2,sio,mm);

    k3=step*fn_del(w+0.5*l2);
    l3=step*fn_w(del+0.5*k2,w+0.5*l2,Eqd+0.5*m2,Idc+0.5*o2,2,sio,mm);
    m3=step*fn_Eqd(del+0.5*k2,Eqd+0.5*m2,Efd+0.5*n2,Idc+0.5*o2,2,sio,mm);
    n3=step*fn_Efd(del+0.5*k2,Eqd+0.5*m2,Efd+0.5*n2,Idc+0.5*o2,delo,sio,Idco,2,mm,vref);

```

```

o3=step*fn_Idc(del+0.5*k2,Eqd+0.5*m2,Idc+0.5*o2,2,sio,mm);

k4=step*fn_del(w+l3);
l4=step*fn_w(del+k3,w+l3,Eqd+m3,Idc+o3,2,sio,mm);
m4=step*fn_Eqd(del+k3,Eqd+m3,Efd+n1,Idc+o3,2,sio,mm);
n4=step*fn_Efd(del+k3,Eqd+m3,Efd+n3,Idc+o3,delo,sio,Idco,2,mm,vref);
o4=step*fn_Idc(del+k3,Eqd+m3,Idc+o3,2,sio,mm);

k=(k1+2*k2+2*k3+k4)/6;
l=(l1+2*l2+2*l3+l4)/6;
m=(m1+2*m2+2*m3+m4)/6;
n=(n1+2*n2+2*n3+n4)/6;
o=(o1+2*o2+2*o3+o4)/6;
t=t+step;
del=del+k;
w=w+l;
Eqd=Eqd+m;
Efd=Efd+n;
if(Efd>=5)
    Efd=5;
end
if(Efd<=-5)
    Efd=-5;
end
Idc=Idc+o;
Pe=0;
const=VB*cos(del) - c*XLB*Idc*cos(sio);
Itld=-const/(Xtl + XLB);
Itlq=0;
mm=-mat_K*[del-delo;w-wo;Eqd-Eqod;Efd-Efdo;Idc-Idco] + mmo;
if(mm>1)
    mm=1;
end
if(mm<-1)
    mm=-1;
end
tout = [tout t];
del_out = [del_out del];
w_out = [w_out w];
Eqd_out = [Eqd_out Eqd];
Efd_out = [Efd_out Efd];
Idc_out = [Idc_out Idc];
P_out = [P_out Pe];
mm_out = [mm_out mm];
Q=mm*kk*Idc*((Eqd-(Xdd+Xtl)*Itld)*cos(sio) - (Xq+Xtl)*Itlq*sin(sio));
Q_out=[Q_out Q];
volt_3=abs(Xtl*Itld);
V_out=[V_out volt_3];
end

for ii=0:step:13
k1=step*fn_del(w);
l1=step*fn_w(del,w,Eqd,Idc,1,sio,mm);
m1=step*fn_Eqd(del,Eqd,Efd,Idc,1,sio,mm);
n1=step*fn_Efd(del,Eqd,Efd,Idc,delo,sio,Idco,1,mm,vref);
o1=step*fn_Idc(del,Eqd,Idc,1,sio,mm);

```

```

k2=step*fn_del(w+0.5*11);
l2=step*fn_w(del+0.5*k1,w+0.5*11,Eqd+0.5*m1,Idc+0.5*o1,1,sio,mm);
m2=step*fn_Eqd(del+0.5*k1,Eqd+0.5*m1,Efd+0.5*n1,Idc+0.5*o1,1,sio,mm);
n2=step*fn_Efd(del+0.5*k1,Eqd+0.5*m1,Efd+0.5*n1,Idc+0.5*o1,delo,sio,Idco,1,mm,vref);
o2=step*fn_Idc(del+0.5*k1,Eqd+0.5*m1,Idc+0.5*o1,1,sio,mm);

k3=step*fn_del(w+0.5*12);
l3=step*fn_w(del+0.5*k2,w+0.5*12,Eqd+0.5*m2,Idc+0.5*o2,1,sio,mm);
m3=step*fn_Eqd(del+0.5*k2,Eqd+0.5*m2,Efd+0.5*n2,Idc+0.5*o2,1,sio,mm);
n3=step*fn_Efd(del+0.5*k2,Eqd+0.5*m2,Efd+0.5*n2,Idc+0.5*o2,delo,sio,Idco,1,mm,vref);
o3=step*fn_Idc(del+0.5*k2,Eqd+0.5*m2,Idc+0.5*o2,1,sio,mm);

k4=step*fn_del(w+13);
l4=step*fn_w(del+k3,w+13,Eqd+m3,Idc+o3,1,sio,mm);
m4=step*fn_Eqd(del+k3,Eqd+m3,Efd+n1,Idc+o3,1,sio,mm);
n4=step*fn_Efd(del+k3,Eqd+m3,Efd+n3,Idc+o3,delo,sio,Idco,1,mm,vref);
o4=step*fn_Idc(del+k3,Eqd+m3,Idc+o3,1,sio,mm);
k=(k1+2*k2+2*k3+k4)/6;
l=(l1+2*l2+2*l3+l4)/6;
m=(m1+2*m2+2*m3+m4)/6;
n=(n1+2*n2+2*n3+n4)/6;
o=(o1+2*o2+2*o3+o4)/6;

t=t+step;
del=del+k;
w=w+l;
Eqd=Eqd+m;
Efd=Efd+n;
if(Efd>=5)
    Efd=5;
end
if(Efd<=-5)
    Efd=-5;
end
Idc=Idc+o;
c=mm*kk;
Itlq=(VB*sin(del)+c*XLB*Idc*sin(sio))/XQ;
Itld=(Eqd-VB*cos(del)+c*XLB*Idc*cos(sio))/XD;
Pe=Eqd*Itlq+(Xq-Xdd)*Itlq*Itld;
%-----
mm=-mat_K*[del-delo;w-wo;Eqd-Eqod;Efd-Efd0;Idc-Idco]+mmo;
if(mm>1)
    mm=1;
end
if(mm<-1)
    mm=-1;
end
tout = [tout t];
del_out = [del_out del];
w_out = [w_out w];
Eqd_out = [Eqd_out Eqd];
Efd_out = [Efd_out Efd];
Idc_out = [Idc_out Idc];
P_out = [P_out Pe];
mm_out = [mm_out mm];

```

```

Q=c*Idc*((Eqd-(Xdd+Xtl)*Itld)*cos(sio) - (Xq+Xtl)*Itlq*sin(sio));
Q_out=[Q_out Q];
volt_3=sqrt((Xq+Xtl)*Itlq*(Xq+Xtl)*Itlq + (Eqd-(Xdd+Xtl)*Itld)*(Eqd-(Xdd+Xtl)*Itld));
V_out=[V_out volt_3];
end
subplot(3,2,1);plot(tout,del_out); ylabel('DELTA'); grid on;
subplot(3,2,2);plot(tout,w_out); ylabel('OMEGA'); grid on;
subplot(3,2,3);plot(tout,Eqd_out); ylabel('Eq'); grid on;
subplot(3,2,4);plot(tout,Efd_out); ylabel('Efd'); grid on;
subplot(3,2,5);plot(tout,Idc_out); ylabel('Idc'); grid on;
subplot(3,2,6);plot(tout,P_out); ylabel('Pe'); grid on;

```

B-2 PROGRAM FOR A, B, C, D CALCULATION AND OUTPUT DECISION

\*\*\*\*\*prog2\*\*\*\*\*

```

thss_gauss;
%-----INITIAL CONDITIONS:-----
%-----TRANSMISSION LINE & STATCOM CONSTANTS:-----
XLB=0.3; Xtl=0.3; Ldc=0.6; Rdc=0.000; kk=0.8; mmo=0.5; c=mmo*kk;
%-----RESULTS FROM LOAD FLOWS:-----
VB=1.0; sio=(pi/2-delo+angle(I(3)))-pi; Vto=abs(volt(2)); ILOo=abs(I(3));
%-----MACHINE CONSTANTS:-----
Xq=0.6; Xd=1.0; Xdd=0.3; freq=50; D=0.015; Tdo=5.044; KA=10.0; TA=0.01; H=3.0; M=H/(pi*freq);

%*****

%-----CALCULATION OF INTIAL EXPRESSIONS-----
XD=XLB + Xtl + Xdd;
XQ=XLB + Xtl + Xq;
Idco=ILOo/c;
ILOdo=c*Idco*cos(sio);
ILOqo=c*Idco*sin(sio);
Itlqo=(VB*sin(delo) + c*XLB*Idco*sin(sio))/XQ;
const1=VB*cos(delo)- c*XLB*Idco*cos(sio);
const2=sqrt(Vto^2 - (Xq*Itlqo)^2);
Itldo=(const2 - const1)/(XLB+Xtl);
Eqod=Itldo*Xdd + const2;
VLdo=(Xq+Xtl)*Itlqo;
VLqo=Eqod - (Xdd+Xtl)*Itldo;
Itlo=sqrt(Itldo^2 + Itlqo^2);
ILBdo=(Eqod-VB*cos(delo)+c*XLB*Idco*cos(sio))/XD - c*Idco*cos(sio);
ILBqo=(VB*sin(delo)+c*XLB*Idco*sin(sio))/XQ - c*Idco*sin(sio);
ILBo=sqrt(ILBdo^2 + ILBqo^2);
Peo=Eqod*Itlqo + (Xq-Xdd)*Itlqo*Itldo;
disp('Initial power: ');
disp(Peo);
%-----
id1=VB*sin(delo)/XD;
id3=1/XD;
id5=kk*XLB*mmo*cos(sio)/XD;
id6=kk*XLB*Idco*cos(sio)/XD;

iq1=VB*cos(delo)/XQ;
iq5=kk*XLB*mmo*sin(sio)/XQ;
iq6=kk*XLB*Idco*sin(sio)/XQ;
%-----

```

```

F1=(Xq-Xdd)*Itlqo;
F2=Eqod+(Xq-Xdd)*Itldo;
K21=(F1*id1+F2*iq1);
K23=(F1*id3+Itlqo);
K25=(F1*id5+F2*iq5);
H2=(F1*id6+F2*iq6);
%-----
K31=(Xd-Xdd)*id1;
K33=1 + (Xd-Xdd)*id3;
K35=(Xd-Xdd)*id5;
H3= (Xd-Xdd)*id6;
%-----
F=Eqod - Xdd*Itldo;
K41=(Xq*Xq*iq1*Itlqo - F*Xdd*id1)/Vto;
K43=F*(1-Xdd*id3)/Vto;
K45=(Xq*Xq*iq5*Itlqo - F*Xdd*id5)/Vto;
H4=(Xq*Xq*iq6*Itlqo - F*Xdd*id6)/Vto;
%-----
F3=kk*(VLdo*cos(sio) + VLqo*sin(sio))/Ldc;
K51=mmo*kk*(cos(sio)*(Xq+Xtl)*iq1 - sin(sio)*(Xdd+Xtl)*id1)/Ldc;
K53=mmo*kk*sin(sio)*XLB/(Ldc*XD);
K55=mmo*kk*(cos(sio)*(Xq+Xtl)*iq5 - sin(sio)*(Xdd+Xtl)*id5)/Ldc -Rdc/Ldc;
H5 =F3 + mmo*kk*(cos(sio)*(Xq+Xtl)*iq6 - sin(sio)*(Xdd+Xtl)*id6)/Ldc;
%-----
A= [ 0      2*pi*freq      0      0      0
     -K21/M    -D/M      -K23/M      0    -K25/M
     -K31/Tdo   0      -K33/Tdo   1/Tdo  -K35/Tdo
     -KA*K41/TA  0      -KA*K43/TA  -1/TA  -KA*K45/TA
     K51      0      K53      0      K55   ];

B= [ 0      -H2/M      -H3/Tdo      -KA*H4/TA   H5]';
EIGEN_A=eig(A)
volt_3=sqrt((Xq+Xtl)*Itlqo*(Xq+Xtl)*Itlqo + (Eqod-(Xdd+Xtl)*Itldo)*(Eqod-(Xdd+Xtl)*Itldo))
%-----
A11=(Itldo*id1 + Itlqo*iq1)/Itlo;
A13=Itldo*id3/Itlo;
A15=(Itldo*id5 + Itlqo*iq5)/Itlo;
B1=(Itldo*id6 + Itlqo*iq6)/Itlo;
%-----
A21=(ILBdo*id1 + ILBqo*iq1)/ILBo;
A23=ILBdo*id3/ILBo;
A25=(ILBdo*(id5-kk*mmo*cos(sio)) + ILBqo*(iq5-kk*mmo*sin(sio)))/ILBo;
B2=(ILBdo*(id6-kk*Idco*cos(sio)) + ILBqo*(iq6-kk*Idco*sin(sio)))/ILBo;
%-----
A31=K21;
A33=K23;
A35=K25;
B3=H2;
%-----
F4=Eqod - 2*(Xdd+Xtl)*Itldo;
F5=-2*(Xq+Xtl)*Itlqo;
A41=F4*id1+F5*iq1;
A43=Itldo+id3*F4;
A45=F4*id5+F5*iq5;
B4=F4*id6+F5*iq6;

```



```

% %-----
A51=VB*(sin(delo)*id1 + ILBdo*cos(delo) -ILBqo*sin(delo) + cos(delo)*iq1);
A53=VB*sin(delo)*id3;
A55=VB*(sin(delo)*(id5-kk*mmo*cos(sio)) + cos(delo)*(iq5-kk*mmo*sin(sio)));
B5=VB*(sin(delo)*(id6-kk*Idco*cos(sio)) + cos(delo)*(iq6-kk*Idco*sin(sio)));
% %-----
A61=VB*(-iq1*sin(delo)+id1*cos(delo)-ILBqo*cos(delo)-ILBdo*sin(delo)) + 2*XLB*A21;
A63=VB*cos(delo)*id3 + 2*XLB*A23;
A65=VB*(-sin(delo)*(iq5-kk*mmo*sin(sio))+cos(delo)*(id5-kk*mmo*cos(sio))) + 2*XLB*A25;
B6=VB*(-sin(delo)*(iq6-kk*Idco*sin(sio))+cos(delo)*(id6-kk*Idco*cos(sio))) + 2*XLB*A25;
% %-----
%
C1= [A11 0 A13 0 A15]; D1= [B1]; %-----delta Itl
C2= [A21 0 A23 0 A25]; D2= [B2]; %-----delta ILB
C3= [A31 0 A33 0 A35]; D3= [B3]; %-----delta P1
C4= [A41 0 A43 0 A45]; D4= [B4]; %-----delta Q1
C5= [A51 0 A53 0 A55]; D5= [B5]; %-----delta P2
C6= [A61 0 A63 0 A65]; D6= [B6]; %-----delta Q2
%
% %-----
if(max(real(EIGEN_A))>0)
    disp('SYSTEM IS UNSTABLE');
else
    sys_1=ss(A,B,C1,D1); zero_1=zero(sys_1); pole_1=pole(sys_1); G1=dcgain(sys_1);
    sys_2=ss(A,B,C2,D2); zero_2=zero(sys_2); pole_2=pole(sys_2); G2=dcgain(sys_2);
    sys_3=ss(A,B,C3,D3); zero_3=zero(sys_3); pole_3=pole(sys_3); G3=dcgain(sys_3);
    sys_4=ss(A,B,C4,D4); zero_4=zero(sys_4); pole_4=pole(sys_4); G4=dcgain(sys_4);
    sys_5=ss(A,B,C5,D5); zero_5=zero(sys_5); pole_5=pole(sys_5); G5=dcgain(sys_5);
    sys_6=ss(A,B,C6,D6); zero_6=zero(sys_6); pole_6=pole(sys_6); G6=dcgain(sys_6);
% %-----
sy_1=pck(A,B,C1,D1);
sy_2=pck(A,B,C2,D2);
sy_3=pck(A,B,C3,D3);
sy_4=pck(A,B,C4,D4);
sy_5=pck(A,B,C5,D5);
sy_6=pck(A,B,C6,D6);
mat=zeros(1,6);
cnt=0;
for ii=1:5
    if(real(zero_1(ii))>=0)
        cnt=cnt+1;
    end
end
if(cnt>=1)
    mat(1,1)=1;
    fprintf('system 1 has %d right half plane zeros\n',cnt);
else
    fprintf('system 1 has no right half plane zeros\n');
end
% %-----
cnt=0;
for ii=1:5
    if(real(zero_2(ii))>=0)
        mat(1,2)=1;
        cnt=cnt+1;
    end
end

```

```

end
if(cnt>=1)
    fprintf('system 2 has %d right half plane zeros\n',cnt);
else
    fprintf('system 2 has no right half plane zeros\n');
end
% %-----
cnt=0;
for ii=1:5
    if(real(zero_3(ii))>=0)
        mat(1,3)=1;
        cnt=cnt+1;
    end
end
if(cnt>=1)
    fprintf('system 3 has %d right half plane zeros\n',cnt);
else
    fprintf('system 3 has no right half plane zeros\n');
end
% %-----
cnt=0;
for ii=1:5
    if(real(zero_4(ii))>=0)
        mat(1,4)=1;
        cnt=cnt+1;
    end
end
if(cnt>=1)
    fprintf('system 4 has %d right half plane zeros\n',cnt);
else
    fprintf('system 4 has no right half plane zeros\n');
end
% %-----
cnt=0;
for ii=1:5
    if(real(zero_5(ii))>=0)
        mat(1,5)=1;
        cnt=cnt+1;
    end
end
if(cnt>=1)
    fprintf('system 5 has %d right half plane zeros\n',cnt);
else
    fprintf('system 5 has no right half plane zeros\n');
end
% %-----
cnt=0;
for ii=1:5
    if(real(zero_6(ii))>=0)
        mat(1,6)=1;
        cnt=cnt+1;
    end
end
if(cnt>=1)
    fprintf('system 6 has %d right half plane zeros\n',cnt);
else

```

```

    fprintf('system 6 has no right half plane zeros\n');
end
% %-----
hsv=zeros(6,6);
[w11,w12]=sysbal(sy_1);
[w21,w22]=sysbal(sy_2);
[w31,w32]=sysbal(sy_3);
[w41,w42]=sysbal(sy_4);
[w51,w52]=sysbal(sy_5);
[w61,w62]=sysbal(sy_6);
hsv=[w12 w22 w32 w42 w52 w62];
% %-----
fprintf('\n\tHANKEL SINGULAR VALUES FOR THE %d SYSTEMS FOR WHICH THERE ARE NO RHP
ZEROS.\n',6-(mat(1,1)+mat(1,2)+mat(1,3)+mat(1,4)+mat(1,5)+mat(1,6)));
fprintf('\n');
for ii=1:6
    if(mat(1,ii)~=1)
        fprintf('\tSYSTEM %d',ii);
    end
end
fprintf('\n');
for ii=1:6
    if(mat(1,ii)~=1)
        fprintf('\t%f',max(hsv(1,ii)));
    end
end
end
end

```

### B-3 FUNCTIONS FOR $\delta$ , $\omega$ , $E_d$ , $E_{fd}$ AND $I_{dc}$ CALCULATIONS

\*\*\*\*\**fn\_del*\*\*\*\*\*

```

function f1=fn_del(w);wo=2*pi*50;
f1=w-wo;

```

\*\*\*\*\**fn\_w*\*\*\*\*\*

```

function f2=fn_w(del,w,Eqd,Idc,r,si,mm);wo=2*pi*50;XLB=0.3; Xtl=0.3; Ldc=0.6; Rdc=0.0;
kk=0.8; c=mm*kk;
Xq=0.6; Xd=1.0; Xdd=0.3; freq=50; D=0.015; Tdo=5.044; KA=10.0; TA=0.01; H=3.0; M=H/(pi*freq);
XD=XLB + Xtl + Xdd;
XQ=XLB + Xtl + Xq;
VB=1.0;Pm=1;
if(r==1)
    Itlq=(VB*sin(del)+c*XLB*Idc*sin(si))/XQ;
    Itld=(Eqd-VB*cos(del)+c*XLB*Idc*cos(si))/XD;
end

```

```

if(r==2)
    Itlq=0;
    const=VB*cos(del) - c*XLB*Idc*cos(si);
    Itld=-const/(Xtl + XLB);
end

```

```

Pe=Eqd*Itlq + (Xq-Xdd)*Itlq*Itld;
f2=(Pm-Pe-D*(w-wo))/M;

```

\*\*\*\*\**fn\_Eqd*\*\*\*\*\*

```

function f3=fn_Eqd(del,Eqd,Efd,Idc,r,si,mm);
wo=2*pi*50;XLB=0.3; Xtl=0.3; Ldc=0.6; Rdc=0.0; kk=0.8; c=mm*kk;
Xq=0.6; Xd=1.0; Xdd=0.3; freq=50; Tdo=5.044; KA=10.0; TA=0.01; H=3.0; M=H/(pi*freq);
XD=XLB + Xtl + Xdd;

```

```

XQ=XLB + Xtl + Xq;
VB=1.0;
if(r==1)
    Itld=(Eqd-VB*cos(del)+c*XLB*Idc*cos(si))/XD;
end
if(r==2)
    Itlq=0;
    const=VB*cos(del) - c*XLB*Idc*cos(si);
    Itld=-const/(Xtl + XLB);
end
EI=Eqd + (Xd-Xdd)*Itld;
f3=(Efd-EI)/Tdo;
*****fn_Efd*****
function f4=fn_Efd(del,Eqd,Efd,Idc,delo,sio,Idco,r,mm,vref);
wo=2*pi*50;XLB=0.3; Xtl=0.3; Ldc=0.6; Rdc=0.0; kk=0.8; c=mm*kk;
si=sio;
Xq=0.6; Xd=1.0; Xdd=0.3; Tdo=5.044; KA=10.0; TA=0.01;
XD=XLB + Xtl + Xdd;
XQ=XLB + Xtl + Xq;
VB=1.0;Vto=1;
if(r==1)
    Itlq=(VB*sin(del)+c*XLB*Idc*sin(si))/XQ;
    Itld=(Eqd-VB*cos(del)+c*XLB*Idc*cos(si))/XD;
    vt=sqrt((Xq*Itlq)^2 + (Eqd-Xdd*Itld)^2);
end
if(r==2)
    vt=0;
end
f4=-Efd/TA + KA*(vref-vt)/TA;
*****fn_Idc*****
function f5=fn_Idc(del,Eqd,Idc,r,si,mm);
wo=2*pi*50;XLB=0.3; Xtl=0.3; Ldc=0.6; Rdc=0.000; kk=0.8; c=mm*kk;
Xq=0.6; Xd=1.0; Xdd=0.3; freq=50; Tdo=5.044; KA=10.0; TA=0.01; H=3.0; M=H/(pi*freq);
XD=XLB + Xtl + Xdd;
XQ=XLB + Xtl + Xq;
VB=1.0;
if(r==1)
    vld=(Xq+Xtl)*(VB*sin(del) + c*XLB*Idc*sin(si))/XQ;
    vlq=Eqd-((Xdd+Xtl)*(Eqd-VB*cos(del) + c*XLB*Idc*cos(si))/XD);
    volt3_angle=atan(vlq/vld);
end
if(r==2)
    Itlq=0;
    const=VB*cos(del) - c*XLB*Idc*cos(si);
    Itld=-const/(Xtl + XLB);
    vld=Xtl*Itlq;
    vlq=-Xtl*Itld;
end
f5=c*(vld*cos(si)+vlq*sin(si))/Ldc -Rdc*Idc/Ldc;

```

B-4 PROGRAMFOR POLE PLACEMENT

\*\*\*\*\*pole\_plcmnt\*\*\*\*\*

```
prog2;  
p = 1.1*EIGEN_A;  
q=1.0*EIGEN_A;  
mat_K = place(A,B,p);  
C=C4  
DD=D4;  
mat_L = -1*place(A',C',q);
```